3. RESULTS

3.1 Inhibition of IL-2 secretion by a CD44 receptor globulin and induction of T cell proliferation by cross-linking of CD44

Antigen-specific activation of the influenca HA specific murine T hybridoma IP12-7 has been demonstrated to be highly dependent on the engagement of co-receptors/accessory-receptors, such as CD4 and CD28, provided by the interaction with APCs (Gogol k et al., 1996). Since IP12-7 cells also express CD44 at high level, the system appeared well suited to explore a possible costimulatory function of CD44 in T cell activation by a nominal antigen. The 2PK3 B cell line was used as antigen presenting cells. 2PK3 cells, prepulsed with titrated amounts of influenca HA 317-329 peptide, were mixed with the IP12-7 T cell line at a 1:1 ratio. The mixture was incubated for 24 h. Thereafter T cell activation was accessed by measuring IL-2 secretion (Figure 3). Depending on the presence of a CD44 receptor globulin (CD44-RG), no IL-2 secretion was observed after pulsing with low peptide concentrations. At high peptide concentrations IL-2 production was still reduced by over 40%. This finding confirms that CD44, similar to CD28, can contribute to the antigenic stimulation of T cells.

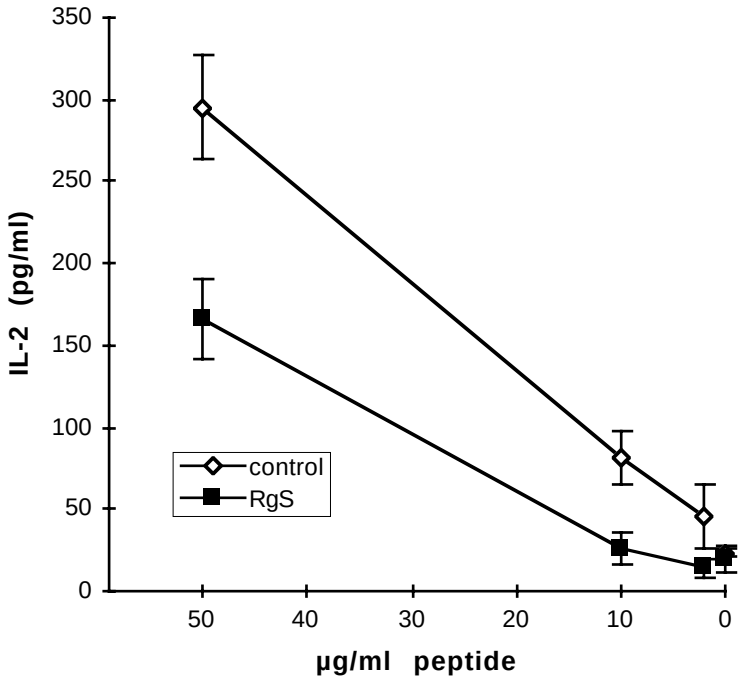

Figure 3: ***A CD44 receptor globulin interferes with antigenic stimulation of a T helper line***
The Th line IP12-7 ($2x10^4$/well) was incubated with 2PK3 cells ($2x10^4$/well), which have been prepulsed with different concentrations of influenca HA317-329 peptide. Cultures contained supernatants of either a CD44-RG producing Ag8 transfectant or of a control transfectant. After 24 h of culture IL-2 secretion was determined in a sandwich ELISA.

Accordingly, cross-linking of CD44 on murine spleen cells (SC) and lymph node cells (LNC) provides a costimulatory signal. Freshly harvested SC were seeded in plates coated with increasing amounts (0-10 g/ml) of anti-CD3. Cross-linking with anti-CD3 mAbs mimics the effect of Ag-TCR/CD3 interaction. Strong proliferative activity, as measured by [^{3}H]thymidin incorporation, was only observed when cells were seeded onto plates coated with high doses of anti-CD3 (10 g/ml). When plates were coated in addition with the CD44s-specific antibody IM7, proliferative activity was also seen in the presence of subthreshold levels of anti-CD3 (1 g/ml). At higher doses of anti-CD3, proliferative activity could not be further augmented by concomitant cross-linking of CD44. Interestingly, the costimulatory effect was only observed with IM7, but not with the CD44s-specific antibody KM81 which occupies the hyaluronic acid binding site of CD44. Cross-linking of CD44v10, which is weakly expressed on SC (R sel et al., 1998), was ineffective (Figure 4). The same results were obtained with freshly isolated LNC (data not shown).

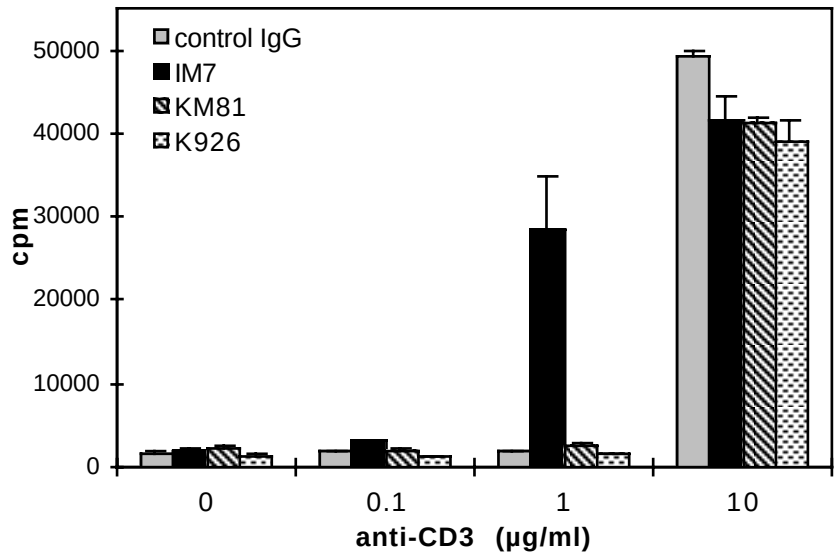

Figure 4

Cross-linkage of CD44 is costimulatory for CD3-induced lymphocyte proliferation
Spleen cells (2x10^5/well) were seeded on plates coated with titrated amounts of anti-CD3 and a constant amount (10 g/ml) of a control antibody, of anti-CD44s (IM7 or KM81) or anti-CD44v10 (K926). Cells were incubated at 37 ¡C for 48 h adding [^{3}H]-thymidine during the last 16 h of culture. Mean values – SD of triplicate cultures are shown.

As demonstrated in the time course of [^{3}H]thymidin uptake (Figure 5A), the costimulatory effect on lymphocyte proliferation by co-engagement of CD3 (low dose) with CD44 was maximal after a culture period of 48 h and declined afterwards.

Induction of proliferation by cross-linking of CD44 at subthreshold levels of CD3 cross-linkage was independent of accessory cells. The same phenomenon seen with unseparated SC and LNC could be observed when purified T cells were cultured on anti-CD3 plus anti-CD44 (IM7) coated plates. Furthermore, the costimulatory activity of CD44 was dose-dependent, i.e. at suboptimal levels of cross-linking of CD3 the proliferation rate of T cells increased according to the level of cross-linking of CD44. However, CD44 by itself did not suffice for inducing cell proliferation, even at high levels of cross-linking (Figure 5B).

To further investigate the mechanism of CD44 mediated costimulation, lymphocytes were stimulated with surrogate antigen presenting cells (APCs), consisting of beads coated with various concentrations of antibody to CD3 (anti-CD3) and/or anti-CD44. These experiments revealed that as a further prerequisite for the costimulatory activity of CD44 it was necessary to cluster CD44 in the vicinity of CD3. No proliferative response was observed, when LNC were incubated with a mixture of beads coated with either low amounts of anti-CD3 or anti-CD44. Yet, beads coated with anti-CD44 plus anti-CD3 (low dose) sufficed for the induction of a proliferative response (Figure 6). The observation, that addition of anti-CD44 antibodies (IM7) to the culture medium did not exert a significant costimulatory effect on anti-CD3(immobilized)-induced spleen cell proliferation (data not shown) adds to the necessity of a spacial vicinity between CD3 and CD44 for costimulatory activity of the latter.

Finally, cross-linking of CD44 had no influence on T cell activation by phorbolesters (e.g. PMA) and calcium ionophore, agents that mimic physiologic T cell activation but bypass early TCR signaling events. As demonstrated in Figure 7A the proliferative response increased according to the amount of PMA and independent of the presence of anti-CD44. Furthermore, in lymphocytes stimulated with suboptimal doses of PMA without ionophore, CD44 ligation could not restore for a calcium signal (Figure 7B).

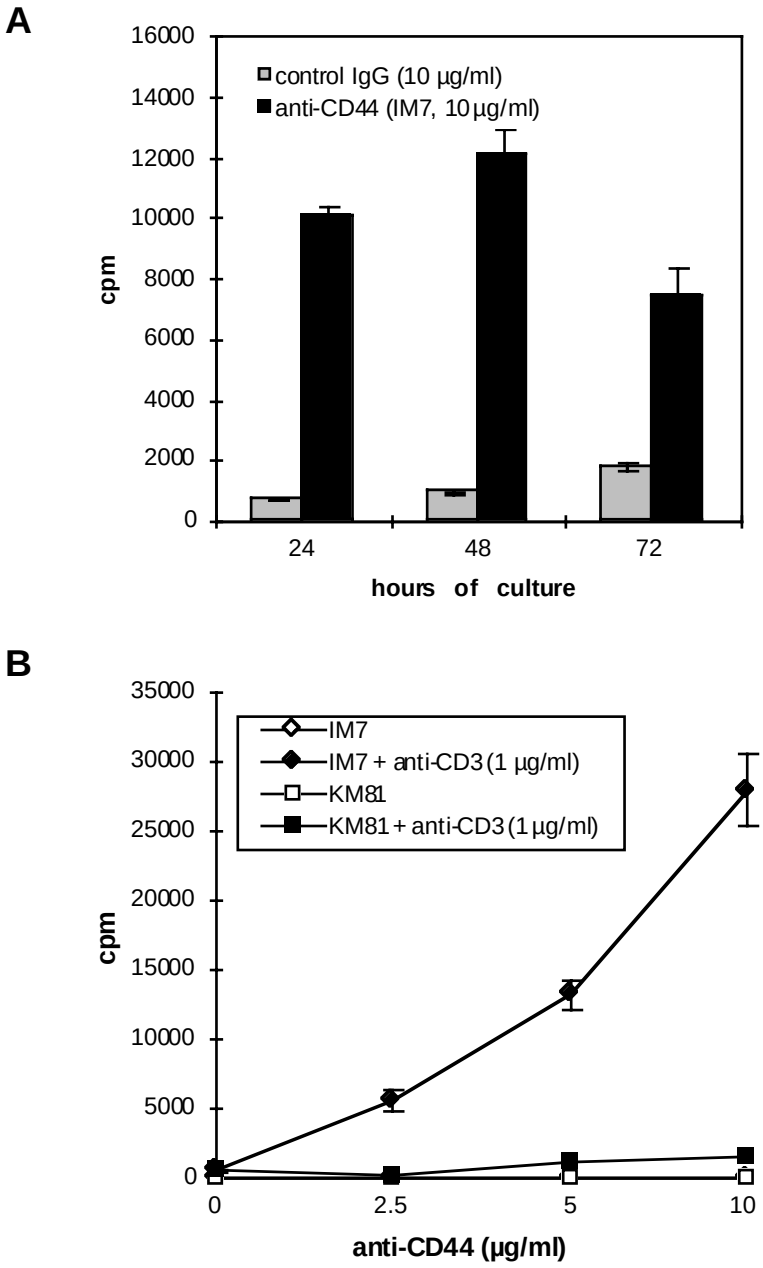

Figure 5

Time kinetics and dose-dependence of CD44-facilitated lymphocyte proliferation
Lymphocytes ($2x10^5$/well) were seeded on plates coated with anti-CD3, anti-CD44 or both anti-CD3 plus anti-CD44. (A) Spleen cells were seeded on plates coated with anti-CD3 (1 g/ml) and a constant amount (10 g/ml) of a control antibody, or of anti-CD44 (IM7). Cultures were maintained for the indicated times adding [^{3}H]-thymidine during the last 16 h of culture. (B) T cell enriched LNC were cultured on plates coated with titrated amounts of anti-CD44 (IM7 or KM81) or with titrated amounts of anti-CD44 plus 1 g/ml anti-CD3. Cells were incubated at 37¡C for 48 h adding [^{3}H]-thymidine during the last 16 h of culture. Mean values – SD of triplicate cultures are shown.

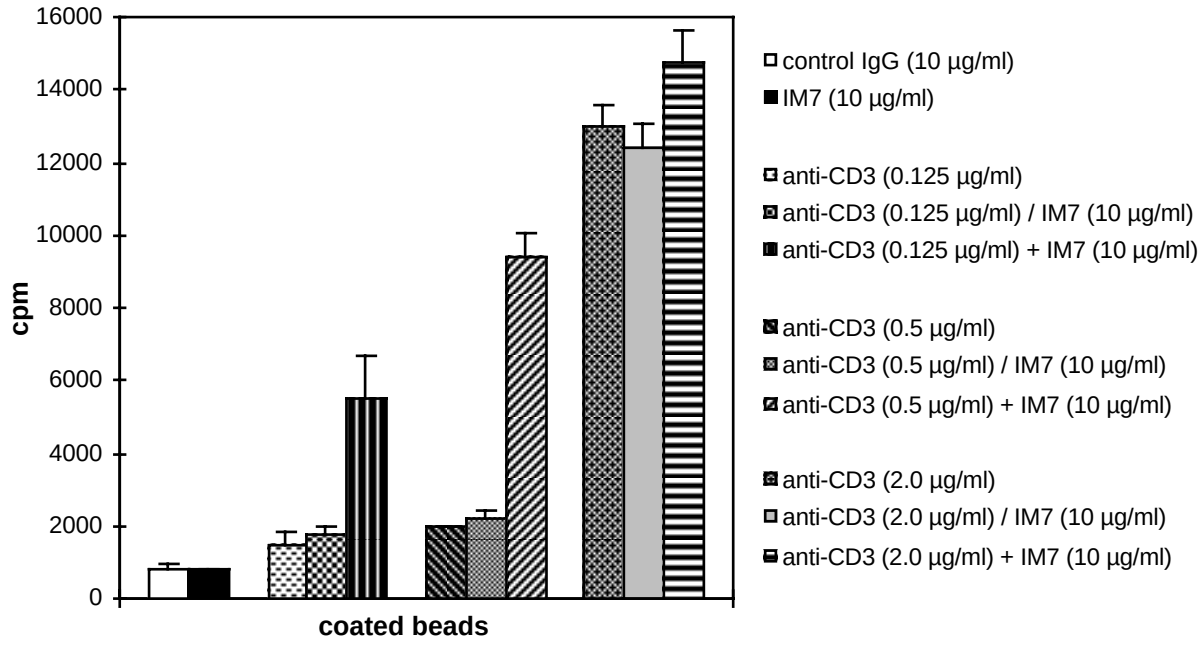

Figure 6
Requirement of proximity between anti-CD44 and anti-CD3 to enhance lymphocyte proliferation
Lymph node cells ($1.5x10^5$/well) were cocultured with beads ($7.5x10^4$/well) coated with either titrated amounts of anti-CD3 or with titrated amounts of anti-CD3 plus a constant amount (10 g/ml) of anti-CD44 (IM7) (anti-CD3 + anti-CD44) or with a mixture of beads coated with either titrated amounts of anti-CD3 or a constant amount (10 g/ml) of anti-CD44 (IM7) (anti-CD3 / anti-CD44). Cells were maintained for 48 h adding [^{3}H]-thymidine during the last 16 h of culture. Mean values – SD of triplicate cultures are shown.

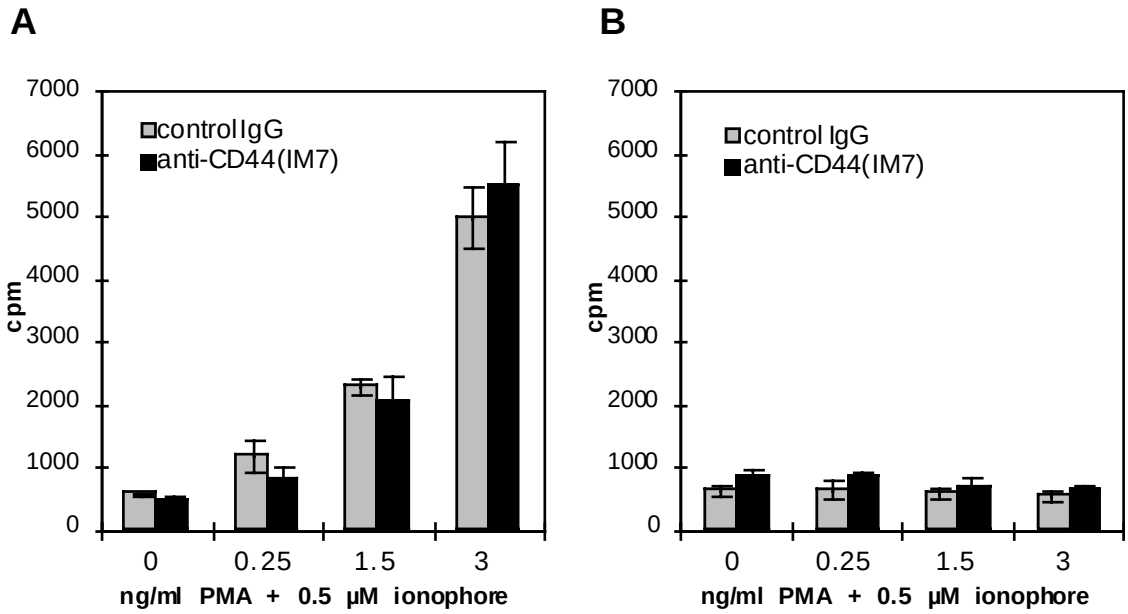

Figure 7

Figure 7 (previous page)
Cross-linkage of CD44 has no influence on T cell stimulation by PMA and ionophore
Spleen cells ($2x10^5$/well) were seeded on plates coated with 10 g/ml of either control IgG or anti-CD44 (IM7). (A) The culture medium contained 0.5 M ionophore and 0-3 ng/ml PMA. (B) The culture medium contained 0-3 ng/ml PMA. Cells were maintained for 48 h adding [^{3}H]-thymidine during the last 16 h of culture. Mean values – SD of triplicate cultures are shown.

The CD44-induced proliferation was accompanied by a profound upregulation of the early T cell activation marker CD69, which has been described as a marker of functional TCR/CD3 triggering (Straus and Weiss, 1992). While cross-linkage of CD44 alone did not result in the induction of CD69 expression on purified murine T lymphocytes, the coimmobilization of anti-CD44 with substimulatory doses of anti-CD3 (0,3 - 1 g/ml) led to a strong increase in CD69 surface expression (Figure 8). CD25, the high avidity α chain of the interleukin-2 (IL-2) receptor, was also clearly upregulated following cross-linkage of CD44 with suboptimal levels of CD3. Again cross-linking of CD44 alone was ineffective (Figure 9). As also observed for lymphocyte proliferation, at high doses of anti-CD3 stimulation (10 g/ml) T cell activation was maximal and neither CD25 nor CD69 expression could be substantially enhanced by additional cross-linkage of CD44. Production of the T cell growth factor interleukin-2 (IL-2), as determined by analysis of culture supernatants, was also significantly augmented by costimulation via CD44 (Figure 10). The costimulatory effect of CD44 cross-linkage on IL-2 production could even be observed at high levels of CD3 stimulation.

Activation of T lymphocytes was accompanied by the formation of blastoid T cells This could be observed in phase contrast microscopy and by flow cytometric analysis of forward scatter (FSC) and side scatter (SSC) signals, parameters which are directly proportional to cell size and granularity, respectively. CD3-induced blast transformation was found to be strongly enhanced following coligation with CD44 (IM7), an effect which was particularly evident at suboptimal levels of CD3 stimulation (Figure 11).

Taken together, these features prove CD44 to be a classical costimulatory molecule. It is worthwhile noting that cross-linking of CD44 was only effective when supporting co-localization of CD44 with the TCR/CD3 complex, since mixtures of beads coated with either anti-CD3 (low dose) or anti-CD44 did not induce T cell activation. Furthermore, induction of costimulatory activity was apparently dependent on the binding site of anti-CD44, as a CD44s-specific antibody occupying the hyaluronic acid binding site displayed no effect.

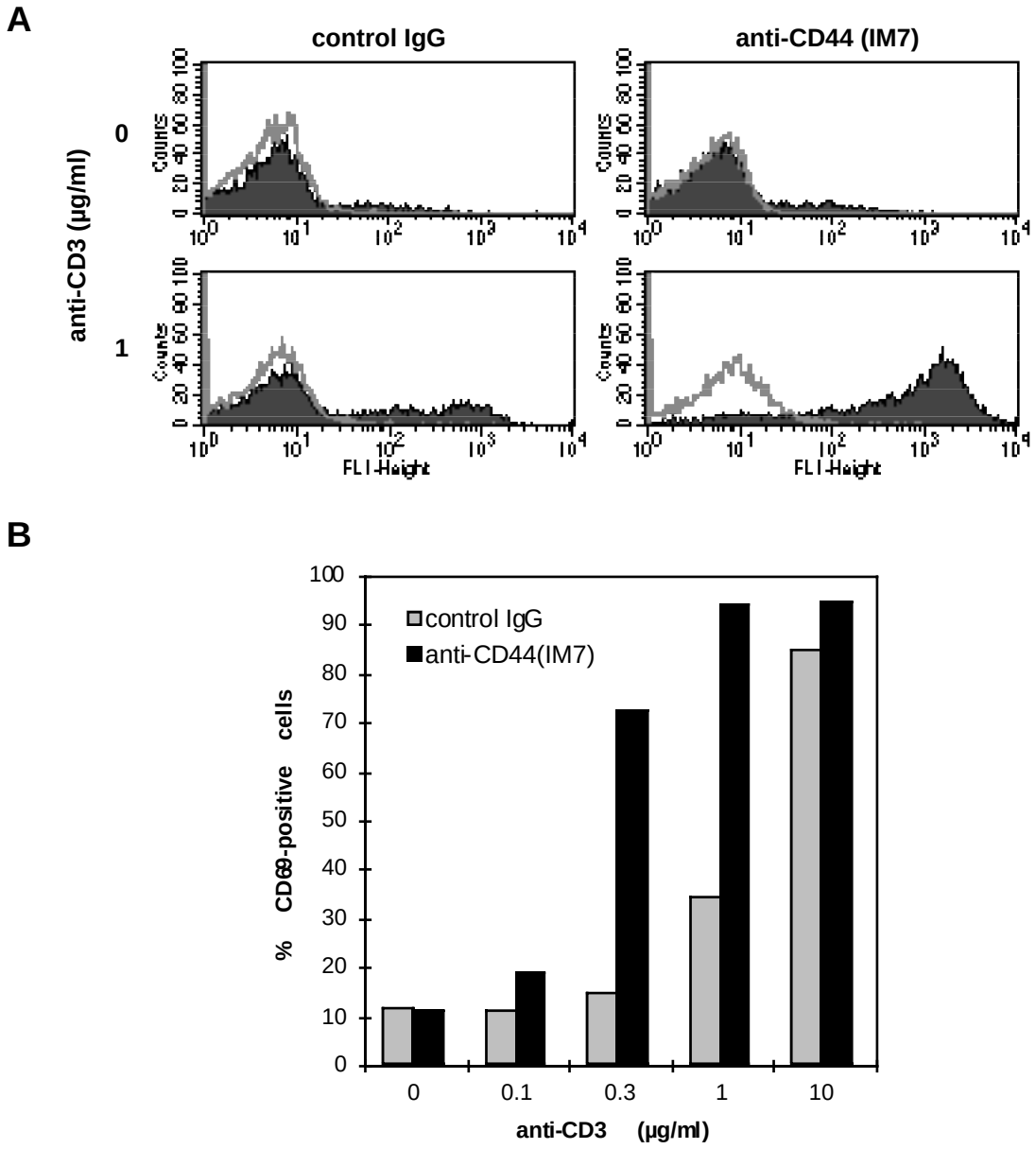

Figure 8

Upregulation of CD69 expression by cross-linking of CD44 and CD3
T cell enriched (nylon wool passage) LNC ($2x10^5$/well) were seeded on plates coated with titrated amounts of anti-CD3 plus 10 g/ml of either control IgG or anti-CD44 (IM7). Surface expression of CD69 was monitored after 12 h of culture by flow cytometric analysis. (A) Single parameter overlays present negative control stainings (grey line) and cells stained with anti-CD69-FITC (filled area), respectively. The percentage of cells stained for CD69 is shown in (B).

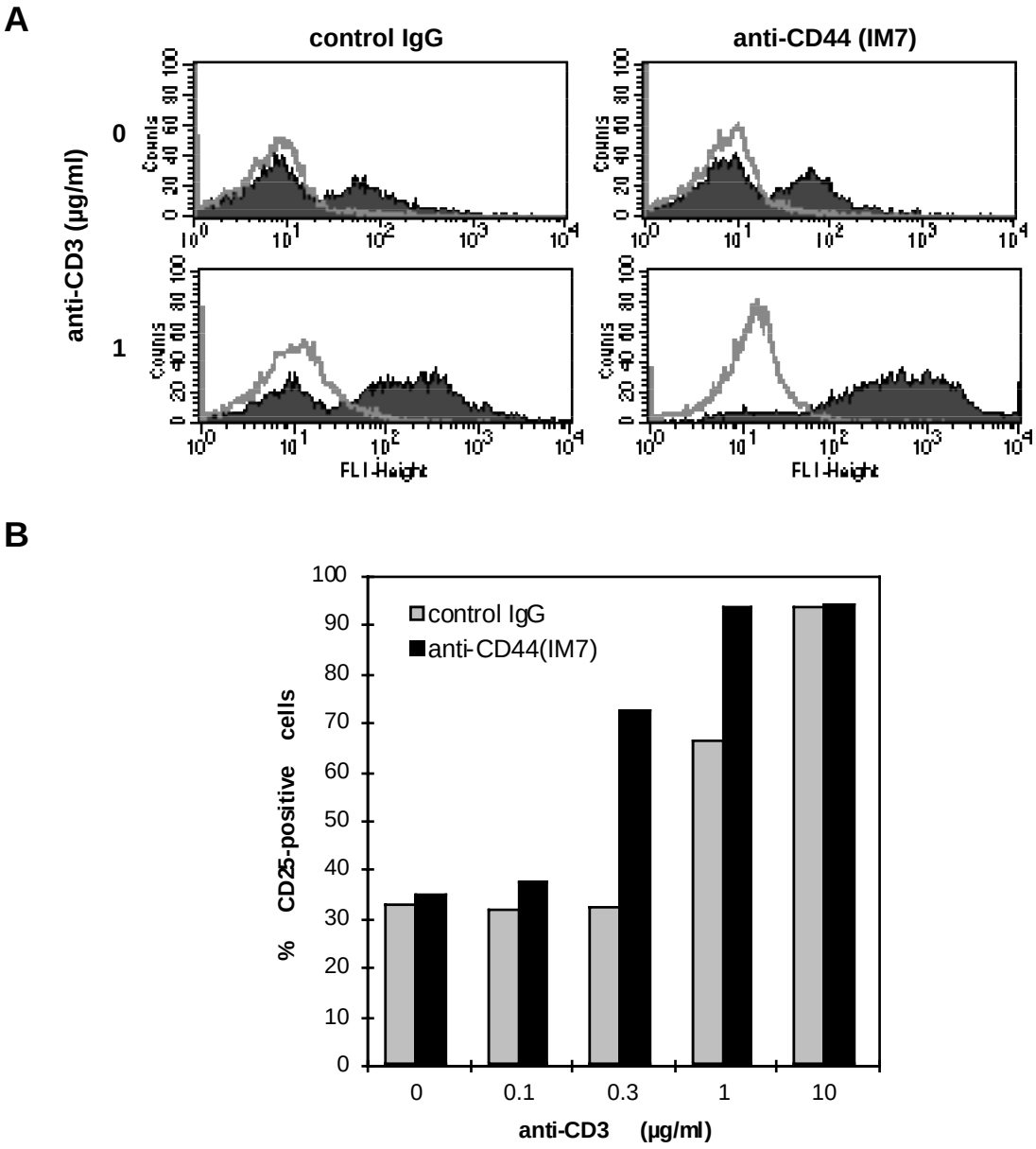

Figure 9

Upregulation of CD25 expression by cross-linking of CD44 and CD3
T cell enriched (nylon wool passage) LNC ($2x10^5$/well) were seeded on plates coated with titrated amounts of anti-CD3 plus 10 g/ml of either control IgG or anti-CD44 (IM7). Surface expression of CD25 was monitored after 48 h of culture by flow cytometric analysis. (A) Single parameter overlays present negative control stainings (grey line) and cells stained with anti-CD25-FITC (filled area), respectively.The percentage of cells stained for CD25 is shown in (B).

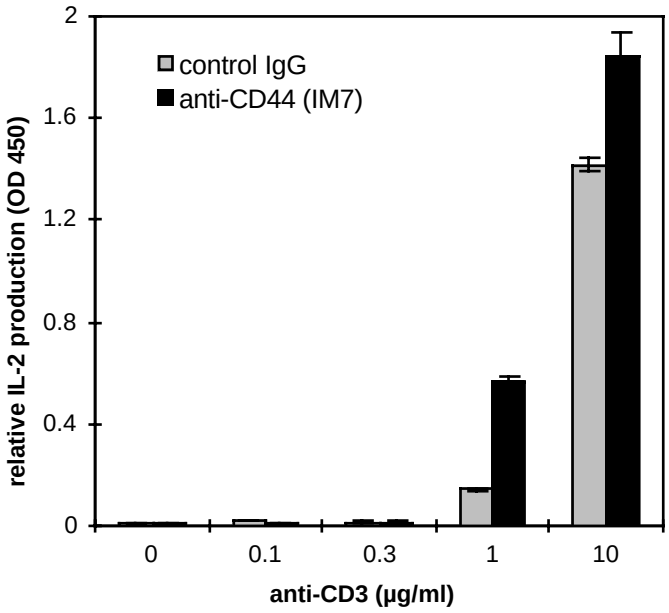

Figure 10: ***Cross-linkage of CD44 is costimulatory for CD3 induced IL-2 production***
T cell enriched (nylon wool passage) LNC ($2x10^5$/well) were seeded on plates coated with titrated amounts of anti-CD3 plus 10 g/ml of either control IgG or anti-CD44 (IM7). The relative production of IL-2 was estimated by a cytokine ELISA from supernatants harvested after 48 h of culture. The optical density (OD) at 450 nm is shown. Results are expressed as the mean OD – SD of triplicate cultures.

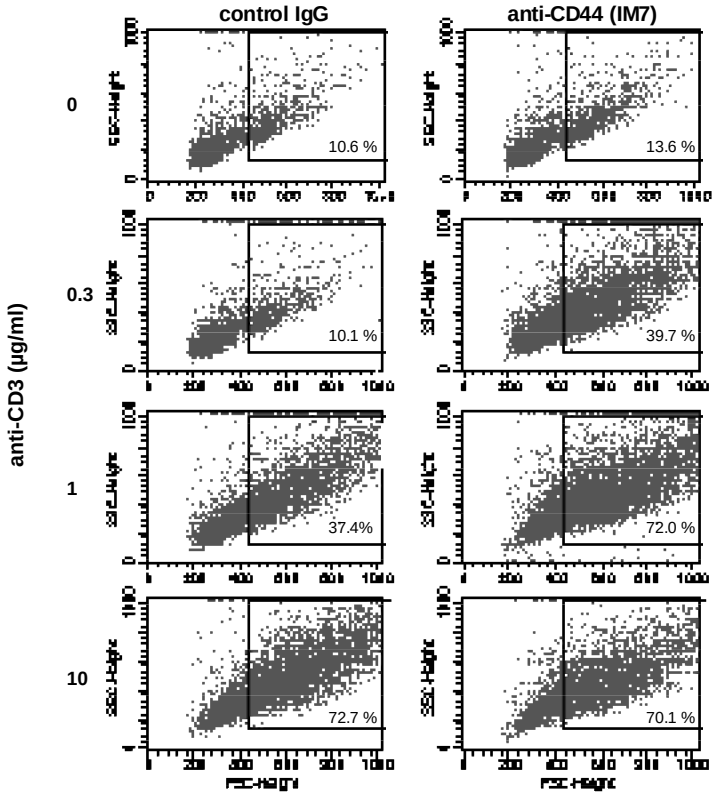

Figure 11

Figure 11 (previous age): ***Upregulation of blast transformation by cross-linking of CD44 and CD3***
T cell enriched (nylon wool passage) LNC ($2x10^5$/well) were seeded on plates coated with titrated amounts of anti-CD3 plus 10 g/ml of either control IgG or anti-CD44 (IM7). After 48 h of culture, cells were analyzed by flow cytometry. Forward scatter (FSC) / side scatter (SSC) patterns are shown. Blastoid cells are located in the inserted quadrant. The percentage of blasts is indicated.

3.2 Induction of apoptosis by cross-linking of CD44

Cross-linking of CD3 has been described to induce T cell activation or T cell death depending on the state of T cell maturation (Smith et al., 1989) and induction of apoptosis by anti-CD3 also is facilitated by costimulatory molecules (McConkey et al., 1994). Yet, it is still a matter of debate whether the same or distinct costimulatory molecules are engaged in T cell activation and apoptosis. To find a molecule which exerts costimulatory functions in both events would strongly support the idea that costimulatory molecules function as "facilitators" rather than as independent signal transducers. Therefore it was next investigated whether cross-linking of CD44 has an impact on the induction of apoptosis in thymocytes (TC).
TC from newborn mice were cultured for 24 h in plates coated with titrated amounts of anti-CD3 and with IM7 (10 g/ml) or an IgM-specific antibody (331.12, 10 g/ml) antibody as isotype control. If anti-CD3 was coimmobilized with anti-CD44, the number of dead TC, as evaluated by uptake of propidium iodide (PI), was significantly increased (Figure 12A). The decrease in viable cell recovery was due to the induction of apoptotic cell death, as confirmed by annexin V assays. Whereas 39% of TC cultured on anti-CD44 plus anti-CD3 (6 g/ml) coated plates were stained by annexin V-FITC, only 28% and 30% of TC were annexin V positive when cultured on anti-CD44 or anti-CD3 coated plates, respectively. Furthermore, the effect of CD44 cross-linking was even observed at high levels of anti-CD3 stimulation. When plates were coated with 18 g/ml anti-CD3, the percentage of annexin V stained TC increased from 33% to 43% by additional cross-linkage of CD44 (Figure 12B).
Cross-linking of CD44 facilitated induction of apoptosis in TC only in the context with cross-linking of CD3. When TC were cultured for 20 h in the presence of increasing amounts of dexamethasone, a glucocorticoid which is known to induce apoptosis in undifferentiated TC (Wyllie et al., 1980), the percentage of apoptotic cell death increased in a dose dependent manner. Figure 13 demonstrates that dexamethasone induced apoptosis in TC was independent of cross-linking of CD44.

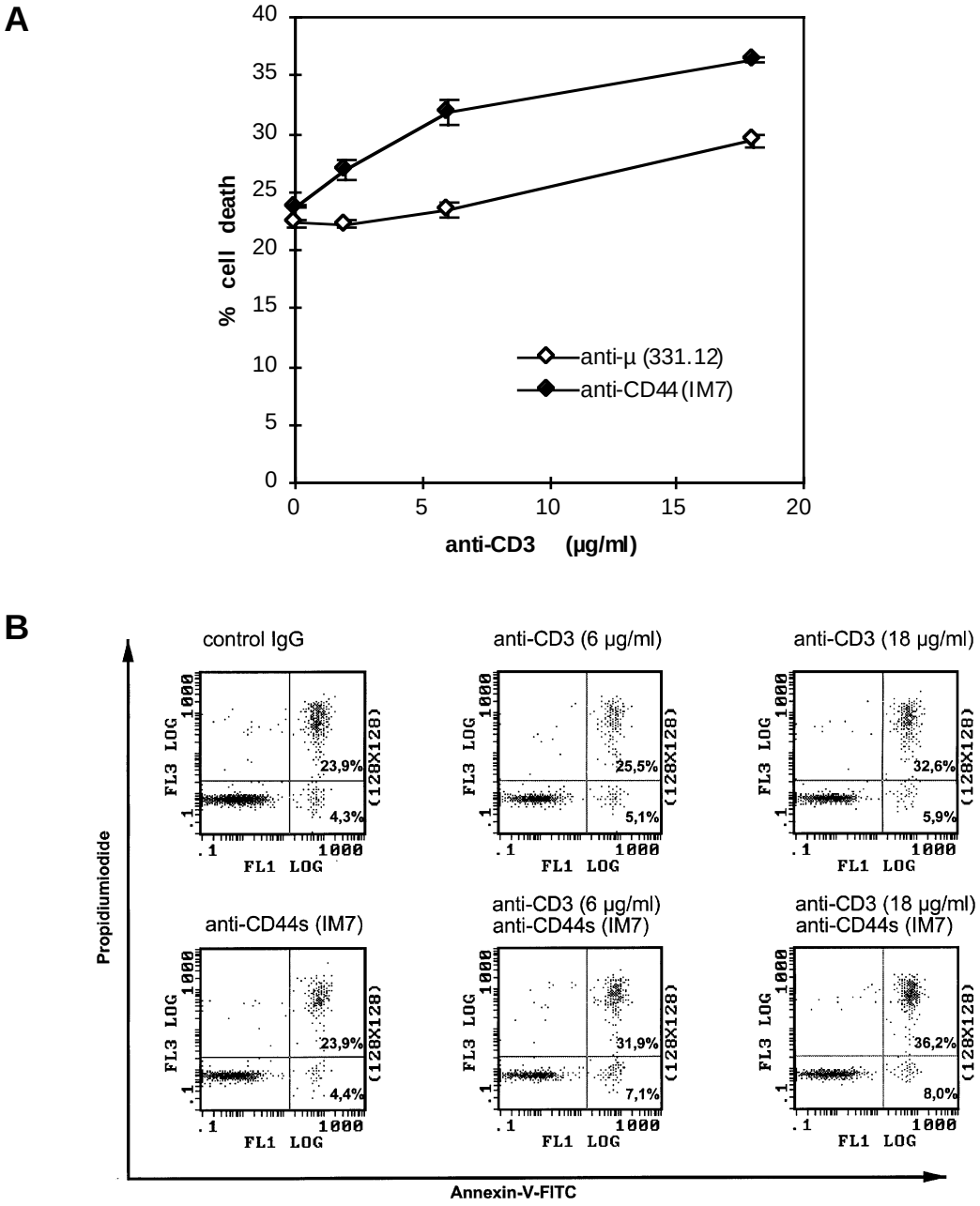

Figure 12

Cross-linkage of CD44 augments CD3-mediated apoptosis in thymocytes
Thymocytes of newborn mice were seeded on plates coated with titrated amounts of anti-CD3 plus 10 g/ml of either control IgG (331.12) or anti-CD44 (IM7). (A) After 20 h of culture, the percentage of dead cells was determined by PI-staining and flow cytometric analysis. Results are expressed as the mean OD – SD of triplicate cultures. (B) Uptake of PI (Y-axis) and staining with annexin V-FITC (x-axis) by thymocytes cultured for 20 h on plates coated with anti-CD3 (0-18 g/ml) plus either a control antibody (331.12) or anti-CD44 (IM7).

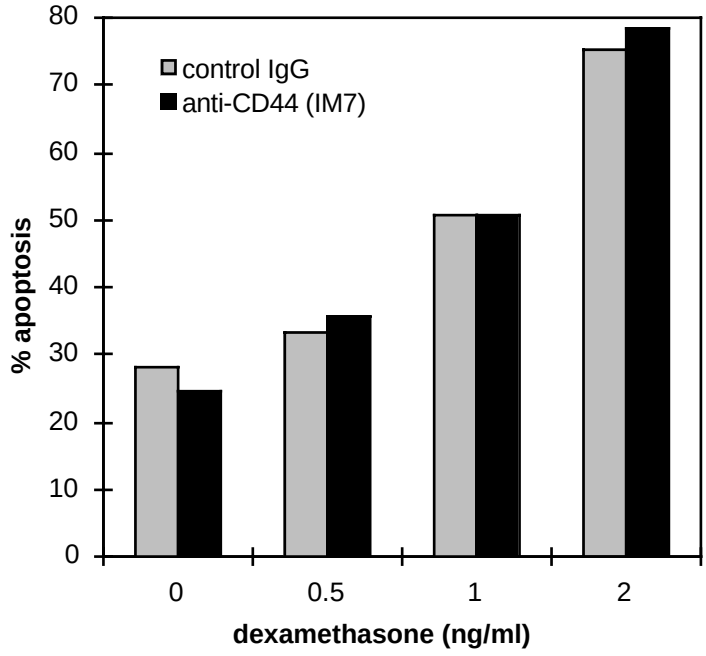

Figure 13: ***Cross-linking of CD44 has no influence on dexamethasone-induced apoptosis of thymocytes***
Thymocytes of newborn mice were seeded on plates coated with either a control antibody (10 g/ml) or anti-CD44 (IM7, 10 g/ml). The culture medium contained titrated amounts of dexamethasone (0-2 ng/ml). Apoptosis was evaluated by flow cytometric analysis of PI-stained nuclei after 20 h of culture.

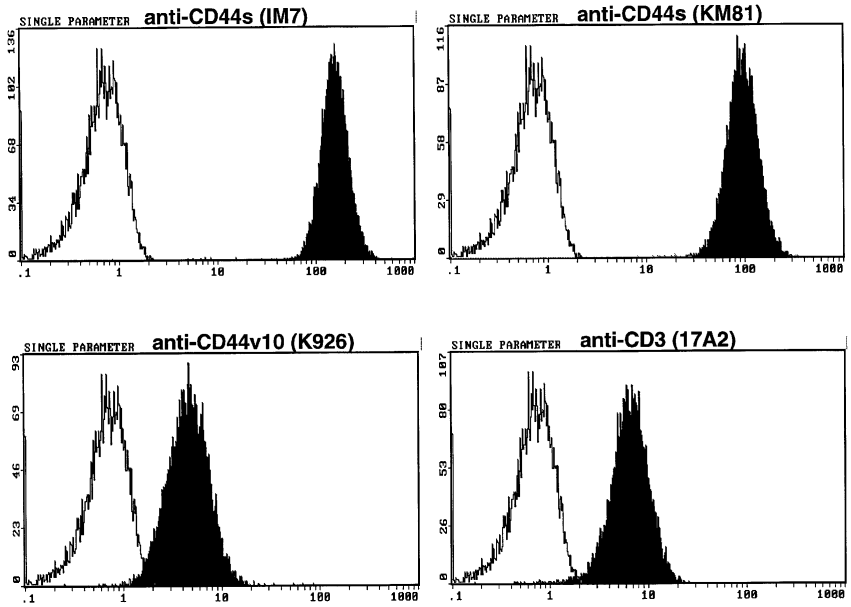

Figure 14: ***Expression of CD44 and CD3 on the Th line IP12-7***
IP12-7 cells were stained with anti-CD44s (IM7 or KM81, anti-CD44v10 (K926) and anti-CD3 (145-2C11). Single parameter overlays of the negative control (second, dye labeled antibody, only) (white area) and of the stained cells (black area) are shown.

The influenza hemagglutinin specific Th clone IP12-7 has been described to express CD44 at a high level (Rajnavolgyi et al., 1994). Notably, the two CD44s-specific antibodies IM7 and KM81 bind with equal efficiency. IP12-7 cells also express CD44v10, although at a lower level than CD44s (Figure 14). Furthermore, it is known that the clone becomes apoptotic upon cross-linking of CD3 in the absence of nominal antigen (Gogolak et al., 1996). Thus, it was interesting to investigate whether cross-linking of CD44 would support induction of apoptosis not only in immature T cells, but also in a T cell line. IP12-7 cells were cultured for 20 h on plates coated with anti-CD3 in the presence or absence of anti-CD44 mAbs. Figure 15 shows the results of a representative experiment obtained by flow cytometric analysis of PI-labeled nuclei. Upon cross-linking of CD44 at subthreshold amounts of anti-CD3 (1 g/ml), apoptosis, as monitored by the percentage of hypodiploid DNA, was significantly increased. As described for the CD44-induced proliferative activity of peripheral T lymphocytes, induction of apoptosis in the IP12-7 line was dependent on the binding site of the CD44-specific antibody, i.e. it was not observed with KM81 nor with K926 (Figure 15B). Also, cross-linking of CD44 by itself exerted no effect. The synergistic increase and acceleration of TCR/CD3-mediated programmed cell death by cross-linkage of CD44 could be confirmed by detection of apoptosis in annexin V assays. After 16 h of culture on anti-CD3 coated plates, there was a substantial raise in the percentage of early apoptotic cells (annexin V positive, PI negative) from 11% to 19 %. During the same culture period the percentage of late apoptotic cells (annexin V positive, PI positive) increased from 16% when cultured with CD3 (1 g/ml) plus control antibody to 34% when CD3 (1 g/ml) was coligated with CD44. Again, cross-linking of CD44 by itself was ineffective (Figure 16A). Finally, induction of apoptosis by coligation of CD44 with substimulatory levels of CD3 (1 g/ml) was also observed by DNA fragmentation analysis after agarose gel electrophoresis (Figure 16B).

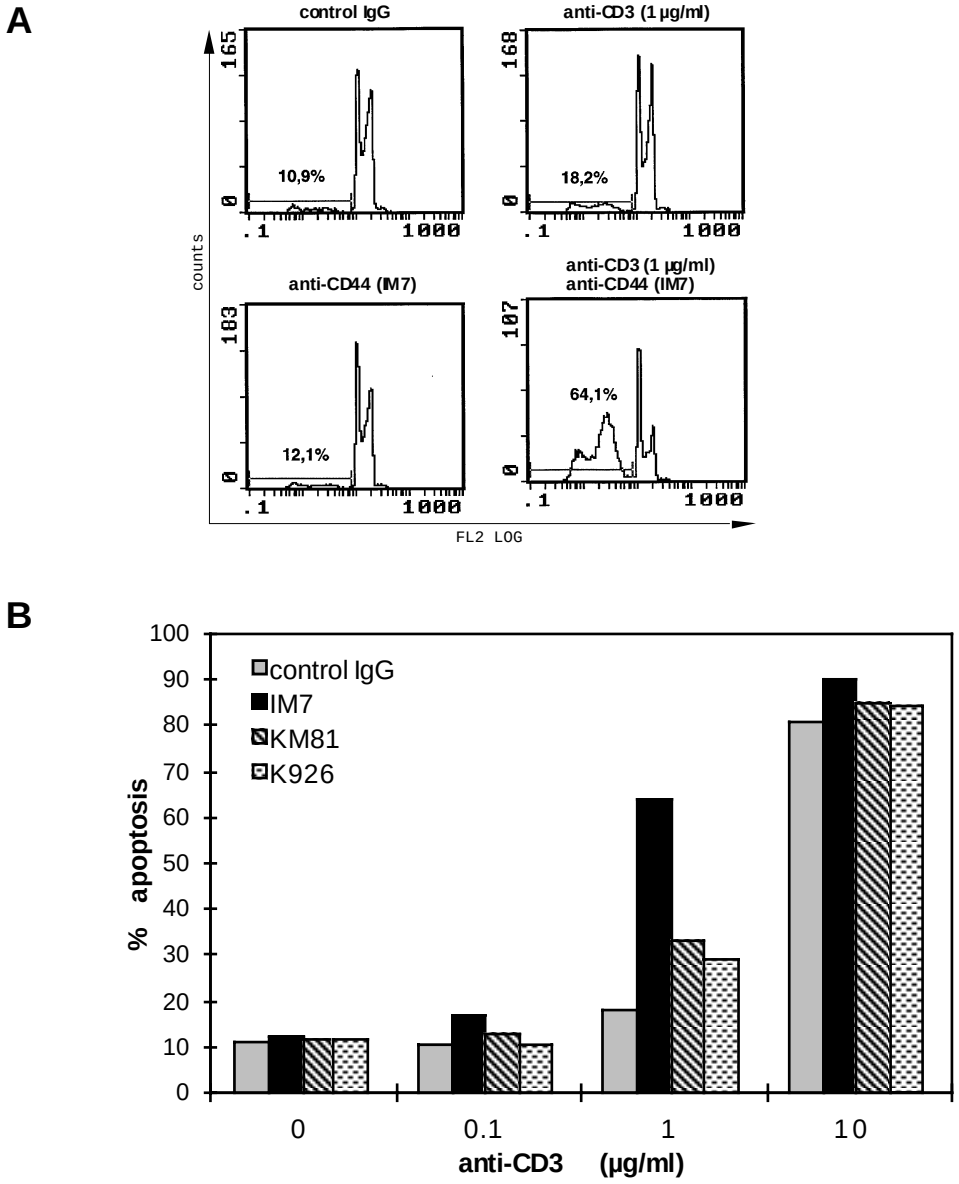

Figure 15

Cross-linkage of CD44 augments CD3-mediated apoptosis in IP12-7 cells
The Th line IP12-7 was cultured on plates coated with anti-CD3, and CD44 or both anti-CD3 plus anti-CD44. (A) Flow cytometric analysis of PI-stained IP12-7 nuclei after 20 h of culture on plates coated with anti-CD3 (0-1 g/ml) plus 10 g/ml of either a control antibody or anti-CD44 (IM7). The percentage of apoptotic nuclei (hypodiploid peak) is indicated in the histograms. (B) Percentage of apoptotic IP12-7 cells as revealed by flow cytometric analysis of PI-stained nuclei after 20 h of culture on plates coated with titrated amounts of anti-CD3 plus 10 g/ml of either anti-CD44s (IM7 or KM81) or anti-CD44v10 (K926).

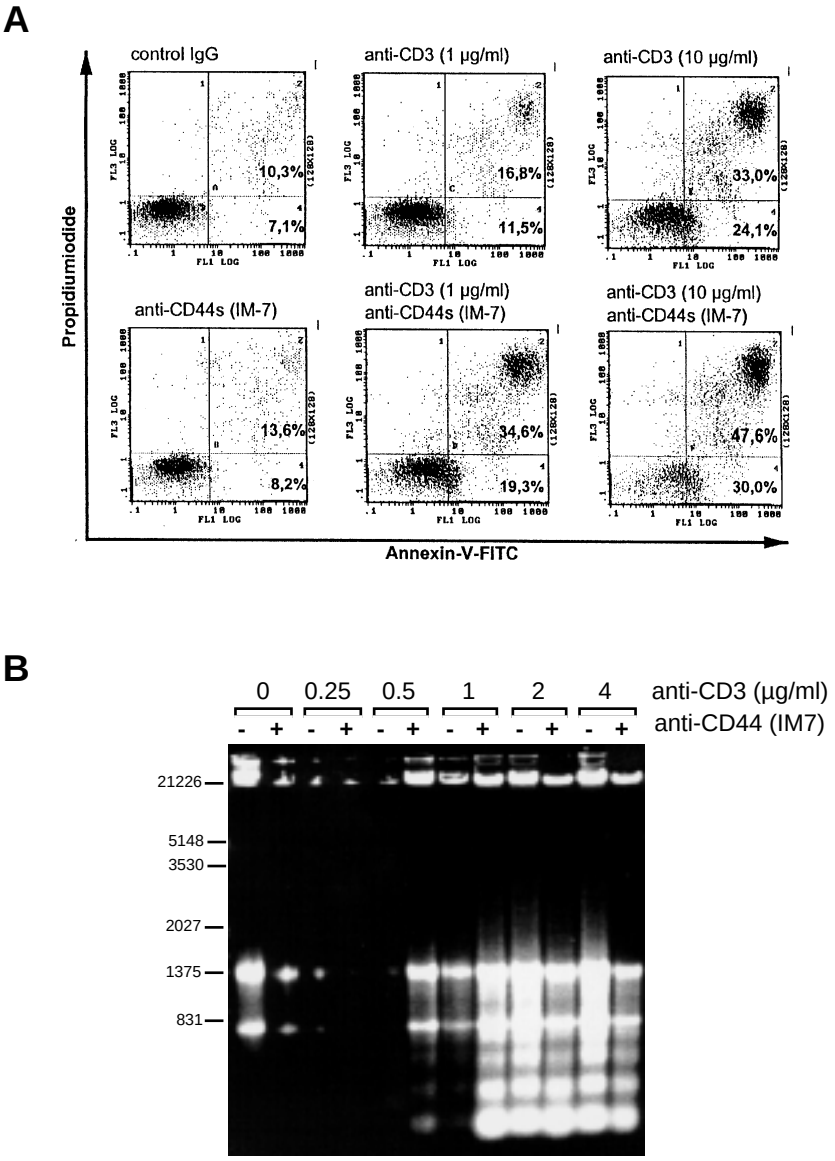

Figure 16

Induction of apoptosis in IP12-7 cells by cross-linking of CD44 and CD3
The Th line IP12-7 was cultured on plates coated with anti-CD3, and CD44 or both anti-CD3 plus anti-CD44. (A) Uptake of PI (Y-axis) and staining with annexin V-FITC (x-axis) by IP12-7 cells cultured for 16 h on plates coated with anti-CD3 (0-10 g/ml) plus 10 g/ml of either a control antibody or anti-CD44. (B) Agarose gel electrophoresis of DNA extracted from IP12-7 cells after 20 h culture in plates coated with titrated amounts of anti-CD3 – anti-CD44 (IM7, 10 g/ml). Positions of molecular weight markers are shown in bp.

CD95-mediated killing has been described to be a major pathway of TCR-mediated apoptosis of T cell hybridomas (Brunner et al., 1995; Ju et al., 1995; Yang et al., 1995). Signaling through the TCR complex leads to upregulation of CD95L, which triggers CD95 to initiate killing. The expression of CD95 and CD95L was examined on anti-CD3 and/or anti-CD44 stimulated cells to determine if they were involved in the effects mediated by anti-CD44 stimulation. Flow cytometric analysis revealed, that induction of apoptosis in IP12-7 cells by cross-linking of CD44 in the presence of low levels of anti-CD3 was accompanied by an increase in CD95 and, more prominent, in CD95L surface expression (Figure 17). Neither CD95 nor CD95L expression was altered by cross-linking CD44 alone. To determine whether the modulation of the CD95/CD95L system has functional impacts on cell death, IP12-7 cells were stimulated to undergo apoptosis in the presence or absence of a blocking anti-CD95 mAb (Jo-2), which prevents the interaction between CD95 and its ligand without inducing apoptosis by itself. Figure 18 demonstrates that the CD95/CD95L interaction is functionally involved in activation induced apoptosis in IP12-7 cells, since CD3 mediated (high dose) apoptosis can be substantially inhibited by the blocking anti-CD95 mAb. Moreover, the "costimulatory" function of CD44 on CD3 (low dose) induced apoptosis was clearly dependent on the CD95/CD95L system.

Thus, initiation of cellular responses by cross-linking of CD44 has been observed under identical conditions in T cell proliferation and T cell apoptosis: i. Cross-linking of CD44 was only efficient at co-engagement of CD3, i.e. cross-linking of CD44 by itself exerted no effect and ii. signal transduction supported by cross-linking of CD44 essentially depended on the binding site of the CD44-specific antibody. Taken together, the data provide evidence for a costimulatory function of CD44 in T cell proliferation and apoptosis by increasing the susceptibility of cells for the induction of TCR-mediated functions without modifying the outcome of the response which would be elicited by stronger TCR triggering in the absence of CD44 costimulation.

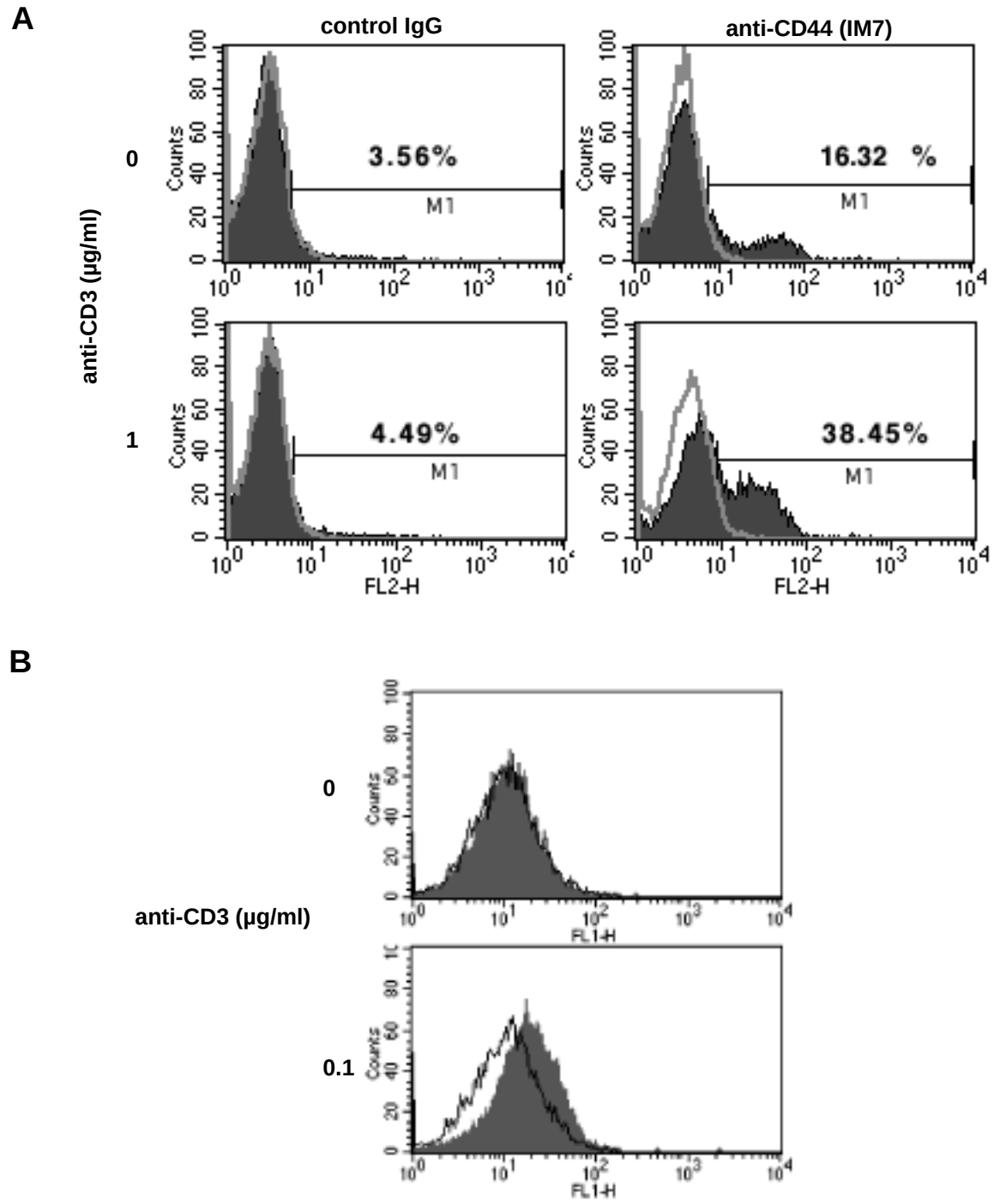

Figure 17

Upregulation of CD95 and CD95L expression upon cross-linkage of CD44 and CD3
IP12-7 cells were cultured for 16 h on plates coated with anti-CD3 plus 10 g/ml of either anti-CD44 (IM7) or control IgG. Expression of CD95L (A) and CD95 (B) was determined by flow cytometry. (A) Single parameter overlays of negative control stainings (grey line) and of cells stained with anti-CD95L-PE (filled area) are shown. (B) Flow cytometric histograms of IP12-7 cells stained with anti-CD95-FITC after 16 h *in vitro* culture on Ab-coated plates. Anti-CD44 stimulated cells are represented by the grey area, while cells treated with control IgG are represented by the black line.

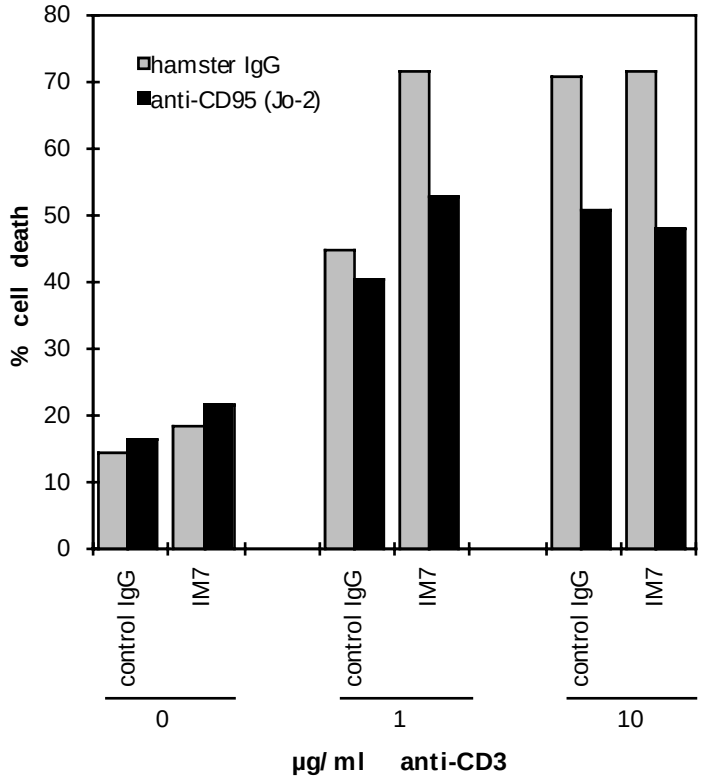

Figure 18

Inhibition of apoptosis induced via cross-linkage of CD3 and CD44 by soluble anti-CD95 mAb
IP12-7 cells were seeded on plates coated with titrated amounts of anti-CD3 plus 10 g/ml of either a control IgG or anti-CD44 (IM7). Cultures were maintained for 20 h in the presence of soluble anti-CD95 (Jo-2, 1 g/ml) or hamster IgG (1 g/ml) as a control. The percentage of dead cells was determined by 7-AAD-staining and flow cytometric analysis.

3.3 CD44 is costimulatory for CD3-induced signal transduction events

To characterize the mechanism by which CD44 contributes to T cell activation, the costimulatory activity of CD44 was analyzed on the level of signal transduction. In current models on costimulation, TCR-induced and independent costimulatory pathways have been suggested to converge at the level of JNK activation (Su et al., 1994; Nun s et al., 1996). However, recent evidence has led to the counterproposal that costimulation might function to amplify the signals transduced by the TCR (Shaw and Dustin, 1997). Therefore, it was investigated whether CD44 induces independent signals required for T cell activation or rather functions to enhances/modify TCR signaling.

3.3.1 Activation of both ERK and JNK pathways after coligation of CD44 with CD3

A first set of experiments was designed to analyze the effect of CD44 costimulation on essential signal transduction cascades involved in T cell activation, namely the p21ras/ERK1/2 and the JNK1/2 pathway. To this end, primary murine T lymphocytes were seeded onto anti-CD44 and/or anti-CD3 coated plates. At the end of the incubation period, whole cellular lysates were prepared, run on a SDS-PAGE and subjected to Western blot analysis.
ERK1/2 activation was evaluated after 30 min of stimulation by immunoblotting using a phospho-specific antibody, that recognizes only catalytically activated ERK1 and ERK2. As shown in Figure 19A (upper panel), no phosphorylation of ERK1/2 was detected in unstimulated T cells or after cross-linking with CD44 alone. CD3 stimulation (10 g/ml anti-CD3) induced a low level of ERK activation that was strongly enhanced by additional cross-linking with anti-CD44 (IM7). The costimulatory activity of CD44 on CD3-induced ERK-phosphorylation was even seen at subthreshold amounts of anti-CD3 (1 g/ml). Similarly to the results on the induction of proliferation and apoptosis, signal transduction supported by CD44 cross-linkage was highly dependent on the binding site of the CD44-specific antibody, i.e. cross-linking with KM81 or K926 was ineffective. Stripping the same blot and reprobing with anti-ERK confirmed that comparable amounts of ERK1 and ERK2 were present in the lysates and that the mode of stimulation had no influence on protein expression (Figure 19A, lower panel).
For the determination of JNK activation cells were stimulated for 180 min on Ab-coated plates. The phosphorylation of c-jun on Ser-63, which is mediated by both activated JNK1 and JNK2, was then analyzed by immunoblotting using a specific antibody. Stimulation with PMA plus ionophore was used as a positive control for c-jun-activation. Similarly to the activation of ERK1/2, CD3-induced phosphorylation of c-jun was found to be upregulated by costimulation via CD44, altough in respect of JNK activation the costimulatory effect was less pronounced at low levels of CD3-stimulation (Figure 19B, upper panel). Again, cross-linking of CD44 by itself was ineffective. Equivalent amounts of c-jun were present in each sample as evaluated after stripping and reprobing the same blot with anti-c-jun (Figure 19B, lower panel).

Taken together, consistent with the effects on the induction of proliferation and apoptosis, these data provide evidence for a cooperation of CD44 with the TCR/CD3-complex for the activation of both ERK and JNK signaling pathways. The reason for such a pleiotropic effect is likely to be that CD44 regulates TCR/CD3 signaling from a very early point.

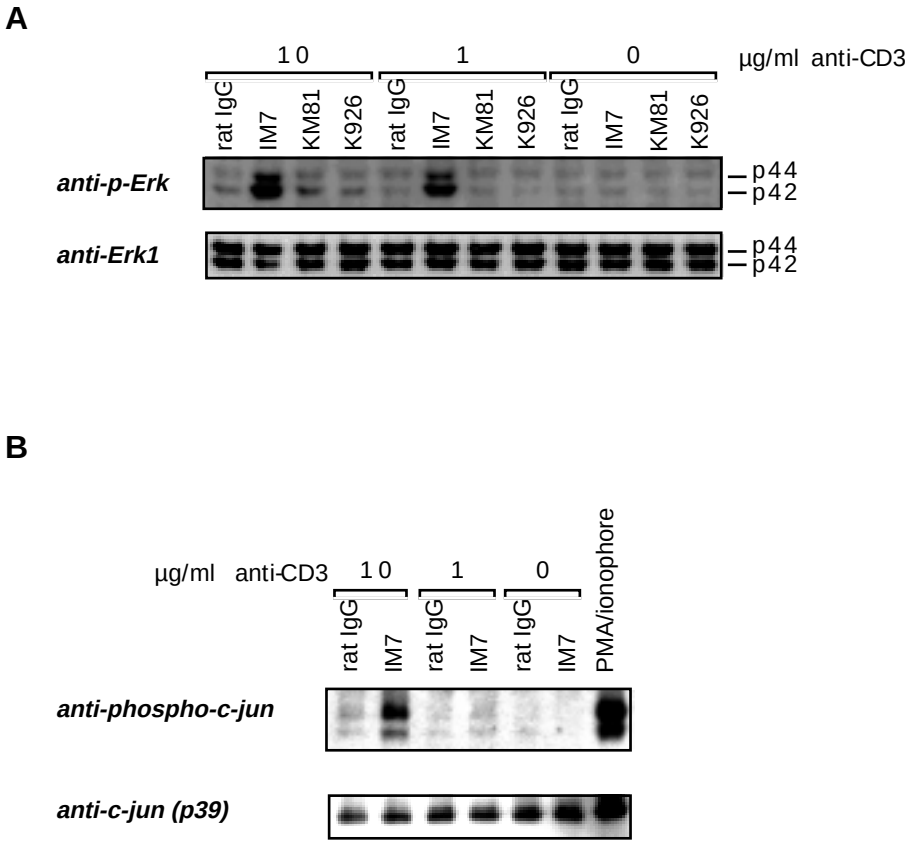

Figure 19: ***Phosphorylation of Erk1/2 and c-jun by cross-linking of CD44 and CD3***
T cell enriched LNC were seeded on plates coated with titrated amounts of anti-CD3 plus 10 g/ml control IgG or anti-CD44s (IM7 or KM81) or anti-CD44v10 (K926). Cells were incubated at 37¡C for 30 min and 180 min, respectively. Lysates of cell stimulated for 30 were subjected to reducing 10% SDS-PAGE, blotted and stained with anti-p-Erk (A, upper panel), lysates of cells stimulated for 180 min were blotted with anti-p-c-jun (B, upper panel). As a positive control for c-jun-phosphorylation, cells were stimulated for 180 min at 37 ¡C with 0.05 g/ml ionophore (A23187) plus 50 ng/ml PMA. The lower panels represent the same blots as in (A) or (B) stripped and reprobed with anti-Erk1 (A) and anti-c-jun (B) Ab.

3.3.2 Cross-linking of CD44 enhances early CD3-induced signaling events

The earliest signaling event induced after engagement of the TCR/CD3 complex is the initiation of a protein tyrosine phosphorylation cascade, which couples TCR-stimulation to the activation of further downstream signaling pathways (Wange and Samelson, 1996; Qian and Weiss, 1997). In consideration of the observation that both ERK, as well as JNK pathways were affected by CD44 costimulation, it was next investigated whether CD44 would also facilitate CD3-induced tyrosine phosphorylation events. Primary murine T lymphocytes were stimulated on plates coated with anti-CD3 and/or anti-CD44 antibodies. After 20 min of incubation, the cells were lysed and phosphoproteins were analyzed on SDS-

PAGE, followed by anti-phosphotyrosine immunoblotting. Cross-linking of CD44 by itself did not stimulate significant tyrosine phosphorylation of cellular substrates. However, when anti-CD44 was coimmobilized with anti-CD3 there was a strong increase in the tyrosine phosphorylation of multiple proteins, as compared to stimulation with anti-CD3 alone (Figure 20A). The induction of tyrosine phosphorylation was particularly evident on proteins with a molecular weight of about 36/38, 59, 76, 95, 120 and 140 kD, a phosphorylation pattern strikingly similar to what has been described following strong TCR-engagement (June et al., 1990; Weiss and Littman 1994). Phosphorylated substrates might therefore include the adaptor proteins LAT (36-38 kD) and SLP-76 and the proto-oncogenes $p95^{vav}$ and $p120^{cbl}$, and phospholipase Cγ (PLCγ), all well known substrates of TCR associated protein tyrosine kinases. Again the costimulatory activity of CD44 was highly dependent on the epitope recognized by the CD44-specific antibody, i.e. costimulation was only observed with IM7, whereas KM81 and K926 were ineffective.

In addition, stripping the blot and reprobing with anti-lck revealed a mobility shift of lck after coligation of CD3 with CD44 (Figure 20B). The activation induced shift in the mobility of lck is known to reflect functional activity of the TCR/CD3 complex (Sancho et al., 1993).

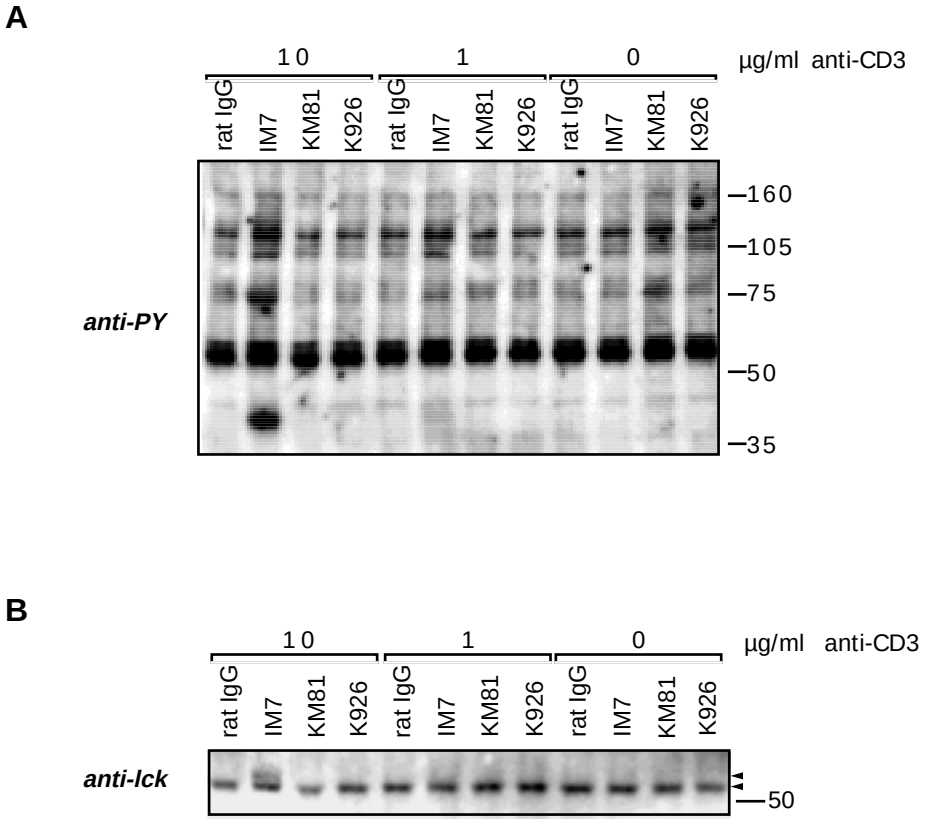

Figure 20

Figure 20 (previuos page)
Coligation of CD44 with CD3 results in increased tyrosine phosphorylation and induces a mobility shift of lck
T cell enriched LNC were seeded on plates coated with titrated amounts of anti-CD3 plus 10 g/ml control IgG or anti-CD44s (IM7 or KM81) or anti-CD44v10 (K926). Cells were stimulated for 20 min at 37 ¡C. After lysis in reducing SDS sample buffer and SDS-PAGE (7.5% polyacrylamide gel), tyrosine phosphorylated proteins were analyzed by immunoblotting with anti-phosphotyrosine Ab (A). The same blot was stripped and reprobed with anti-lck (B). Positions of molecular weight markers are shown in kD.

Signal transduction initiated by CD44 was also evaluated in IP12-7 cells. As described above (section 3.2), this murine Th clone undergoes apoptotic cell death upon CD3-stimulation, an effect which is strongly potentiated by additional cross-linkage of CD44. For the detection of tyrosine phosphorylated proteins, IP12-7 cells were lysed at various times following stimulation on antibody-coated plates and analyzed by Western-blotting using a phosphotyrosine-specific antibody. CD3-stimulation under this experimental conditions was suboptimal, i.e. did not induce strong tyrosine phosphorylation. Also, cross-linkage of CD44 alone exerted no significant effect on the level of tyrosine phosphorylation. However, similarly to the results on primary T cells, tyrosine phosphorylation was markedly increased on a number of cellular proteins by the coengagement of CD3 and CD44. Evaluation of the time kinetics revealed that tyrosine phosphorylation in CD3/CD44 activated cells was induced within minutes and peaked at 10 min after stimulation (Figure 21). Notably, cross-linking of CD3 plus CD44 resulted in sustained signaling, since tyrosine phosphorylation was still found to be upregulated after 30 min of stimulation.
Based on the size of proteins known to be inducibly phosphorylated in response to strong TCR-triggering, it was tempting to speculate that the 95 kD and the 140 kD phosphoproteins were $p95^{vav}$ and phospholipase Cγ (PLCγ), respectively. To prove this assumption, $p95^{vav}$ or PLCγ were immunoprecipitated from cellular lysates of CD44, CD3 or CD3/CD44 stimulated IP12-7 cells. Immunoprecipitates were subjected to SDS-PAGE and tyrosine phosphorylation was analyzed by anti-phosphotyrosine immunoblotting. The coengagement of CD3 and CD44 markedly increased the level of tyrosine phosphorylation of both, $p95^{vav}$ and PLCγ, relative to unstimulated IP12-7 cells or cells stimulated with anti-CD3 (substimulatory) or anti-CD44 (Figure 22). Equal amounts of proteins were precipitated before and after stimulation, as evidenced by stripping and reprobing with antibodies specific for $p95^{vav}$ and PLCγ, respectively. These results indicate that the activity of well known TCR-induced effector enzymes such as PLCγ and $p95^{vav}$, which get activated upon tyrosine phosphorylation, is substantially enhanced in response to CD3/CD44 coligation.

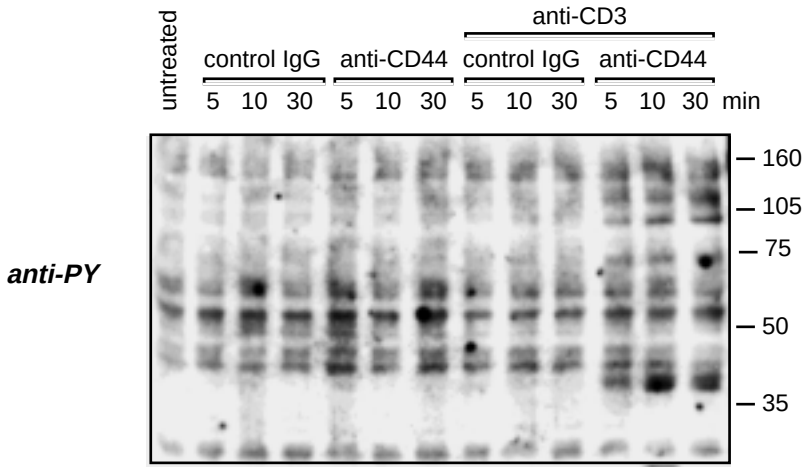

Figure 21

Kinetics of protein tyrosine phosphorylation by cross-linking of CD44 and CD3
IP12-7 cells were cultured for the indicated periods of time at 37 ¡C on plates coated with control IgG (10 g/ml) or anti-CD44 (IM7, 10 g/ml) alone, or anti-CD3 (10 g/ml) plus either control IgG or anti-CD44 (IM7). Total cellular lysates were loaded on a reducing SDS-7.5% polyacryl-amide gel and were analyzed by anti-phosphotyrosine immunoblotting. Positions of molecular weight markers are shown in kD.

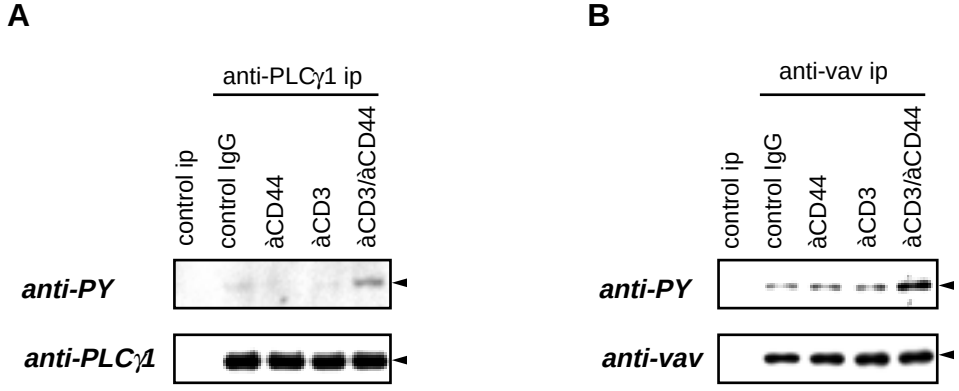

Figure 22

Coligation of CD44 with CD3 results in an increased tyrosine phosphorylation of PLCγ1 and p95^{vav}
IP12-7 cells were stimulated for 10 min at 37 ¡C on plates coated with control IgG (10 g/ml) or anti-CD44 (IM7, 10 g/ml) alone, or anti-CD3 (10 g/ml) plus either control IgG or anti-CD44 (IM7). At the end of the incubation period cells were lysed in RIPA-buffer containing 1% Nonidet P-40 and anti-PLCγ1 (A) or anti-vav (B) immunoprecipitations were performed. Immuno-precipitates (ip) were subjected to reducing 7.5% SDS-PAGE and were analyzed by anti-phospho-tyrosine immunoblotting (upper panels). The lower panels show the same blots stripped and reblotted with anti-PLCγ1 (A) and anti-vav (B), respectively. The positions of PLCγ1 and p95^{vav} are indicated by arrowheads on the right.

One of the most striking changes in tyrosine phosphorylation elicited by strong TCR engagement is the rapid phosphorylation of LAT, a 36/38 kD transmembrane adaptor protein which is essential for coupling the TCR to the PLCγ-calcineurin-NF-AT and the ras-MAPK-AP1 pathways (Finco et al., 1998). LAT is targeted to the glycolipid-enriched microdomains (GEMs) via palmitoylation. This subcellular localization is required for effective T cell activation (Lin et al., 1999). Density gradient ultracentrifugation of detergent (Triton X-100) cell lysates and subsequent anti-phosphotyrosine immunoblotting of GEM and Triton X-100 soluble fractions revealed that a significant fraction of the 36/38 kD phosphoprotein heavily phosphorylated on tyrosine residues by coengagement of CD3 and CD44 was found in the GEM fraction (Figure 23; upper panel). By immunoblotting using a LAT-specific antiserum, LAT could be clearly detected in the GEM fractions before and after cell stimulation (Figure 23; lower panel). Importantly, the 36/38 kD phosphoprotein and LAT were found to comigrate. The finding that the intensity of the LAT specific band in the GEM fraction decreased after coligation of CD3 and CD44 is likely due to an adverse effect of the phosphorylation of LAT on the binding capacity of the antiserum, as it has been described by Brdicka et al., 1998. This data demonstrate the presence of LAT in the GEMs of IP12-7 cells and strongly indicate that the 36/38 kD phosphoprotein detectable in CD3/CD44 stimulated T cells is identical to tyrosine phosphorylated LAT.

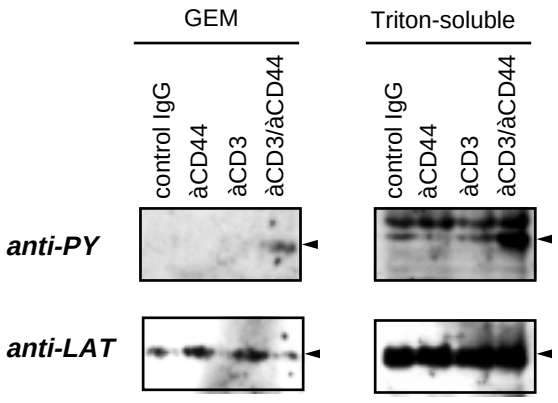

Figure 23: ***Partition of LAT into GEMs and analysis of tyrosine phosphorylation in GEM and Triton X-100 soluble fractions following cross-linking of CD44 and CD3***
IP12-7 cells were stimulated for 15 min at 37 ¡C on plates coated with control IgG (10 g/ml) or anti-CD44 (IM7, 10 g/ml) alone, or anti-CD3 (10 g/ml) plus either control IgG or anti-CD44 (IM7). Cells were lysed in TNE-buffer containing 0.5% Triton X-100 and subjected to sucrose gradient ultracentrifugation. Twelve fractions were collected from the top. GEM-fractions (pooled fractions 2-4) and Triton X-100 soluble fractions (pooled fractions 10-12) were resolved by reducing 10% SDS-PAGE and immunoblotted with anti-phosphotyrosine mAb (upper panel). The lower panel shows the same blot stripped and reprobed with anti-LAT Ab. The position of LAT is indicated by an arrowhead on the right.

Thus, CD44 "signaling" generally required coengagement of the TCR and resulted in an amplification of well known TCR-mediated signals. These features strongly suggest that CD44 exerts its costimulatory function by enhancing signal transduction via the TCR/CD3 complex, rather than initiating a TCR/CD3 complex independent signaling cascade.

To strengthen this interpretation proximal TCR-induced signaling events were evaluated. Antigen receptor engagement results in the rapid association of the protein tyrosine kinase ZAP-70 with the TCR-complex. This permits the tyrosine phosphorylation and activation of ZAP-70, which then phosphorylates its downstream substrates, including LAT and SLP-76 (Chan et al., 1992; Bubeck-Wardenburg et al., 1996; Zhang et al., 1998). Thus, activation of ZAP-70 plays a central role in coupling the initial triggering event to downstream signaling cascades. To examine the influence of CD44 cross-linkage on TCR-mediated activation of ZAP-70, cell lysates of resting and CD3 or CD3/CD44 activated T lymphocytes were subjected to ZAP-70 immunoprecipitation. ZAP-70 activation was then analysed by SDS-PAGE and anti-phosphotyrosine immunoblotting. Figure 24 (upper panel) shows that in unstimulated and in anti-CD44 treated T cells ZAP-70 was not activated. However, CD3-stimulation induced a low level of tyrosine phosphorylation of ZAP-70, which was found to be strongly upregulated by the coligation of CD3 with CD44. Stripping and reprobing the same blot with anti-ZAP-70 showed that similar amounts of ZAP-70 were immunoprecipitated in all the samples (Figure 24, lower panel).

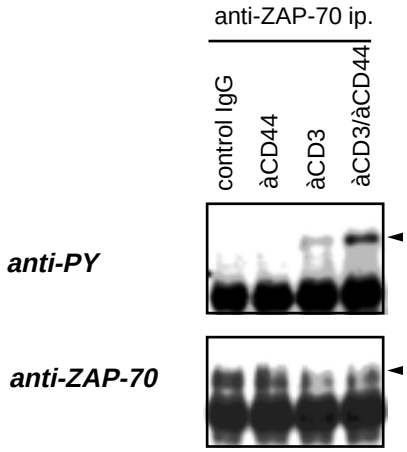

Figure 24: ***Anti-CD44 mAb synergize with and stabilize anti-CD3 induced ZAP-70 phosphorylation***
T cell enriched LNC were stimulated for 10 min at 37 ¡C on plates coated with control IgG (10 g/ml) or anti-CD44 (IM7, 10 g/ml) alone, or anti-CD3 (10 g/ml) plus either control IgG or anti-CD44 (IM7). At the end of the incubation period cells were lysed in RIPA buffer containing 1% Nonidet P-40 and anti-ZAP-70 immunoprecipitations were performed. Immunoprecipitates (ip) were subjected to reducing SDS-PAGE and were analyzed by anti-phosphotyrosine immunoblotting (upper panel). The lower panel shows the same blot stripped and reblotted with anti-ZAP-70. The position of ZAP-70 is indicated by the arrowhead on the right.

The earliest signaling events following engagement of the TCR with antigen involves phosphorylation of TCR subunits, including the ζ chain, at critical signaling motifs termed immunoreceptor tyrosine-based activation motifs (ITAMs). Functional TCR-triggering results also in polarized reorganization of the cytoskeleton and association of the ζ chain with the actin cytoskeleton. Therefore it was next investigated whether cross-linking of CD44 influences TCR-induced ζ chain phosphorylation and cytoskeletal association. The phosphorylation state and subcellular localization of TCR ζ was analyzed in unstimulated and CD3- or CD3/CD44-activated IP12-7 cells. To this end cytosolic and membrane-associated proteins were separated from cytoskeletal-associated proteins using a biochemical fractionation method which is based on their differential solubility in NP-40. Following lysis in 1% NP-40 and centrifugation, cytosolic and membrane proteins are found in the supernatant (Brown, 1993), referred to as the "soluble fraction", whereas cytoskeletal components and associated proteins remain in the pellet. By the use of stronger detergents and sonification, cytoskeletal-associated proteins can be subsequently released from the pellet, referred to as the "insoluble fraction" (Nel et al., 1995). The TCR ζ chain was immunoprecipitated from soluble and insoluble factions and analyzed by SDS-PAGE and anti-phosphotyrosine immunoblotting. Under the experimental conditions applied neither cross-linking of CD44 by itself, nor stimulation of CD3 alone sufficed to upregulate phosphorylation of the TCR ζ chain. But, the coligation of CD3 with CD44 substantially induced tyrosine phosphorylation of TCR ζ, which resulted in its altered migration at 23 kD and reactivity with anti-phosphotyrosine. The appearance of p23 phospho-ζ is characteristic of agonist signaling analyzed in mature T cells (Sloan-Lancaster et al., 1994; Kersh et al., 1998). Importantly, CD3/CD44 coengagement not only enhanced phosphorylation of TCR ζ, but also specifically targeted pp23 ζ to the insoluble fraction (Figure 25; upper panel). Irrespective of the kind of stimulation the unphosphorylated 18 kD isoform of ζ could only be deteced in the soluble fraction, as revealed by anti-ζ immunoblotting (Figure 25; lower panel). These results provide evidence for the contribution of CD44 to TCR ζ-chain phosphorylation and indicate that upon efficient T cell activation by CD3/CD44 coligation phosphorylated ζ specifically associates with the cytoskeleton.

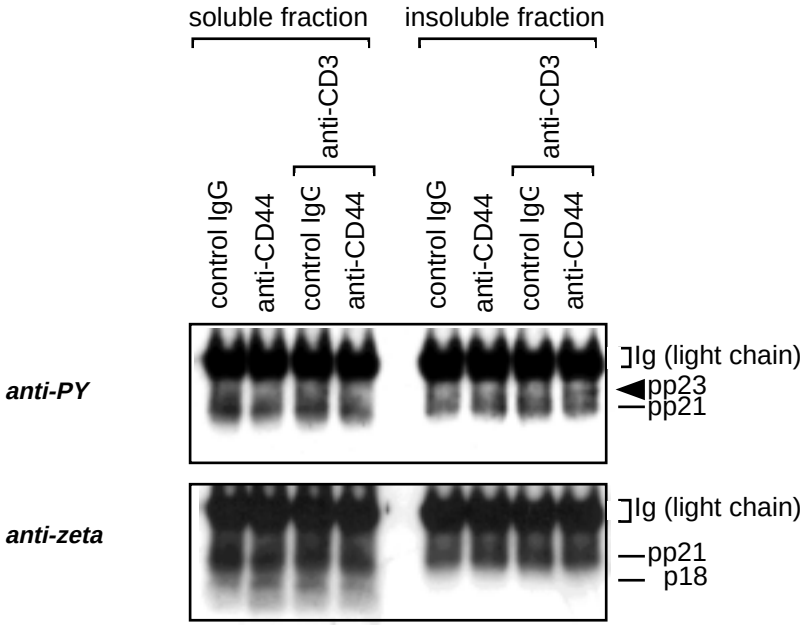

Figure 25: ***Coligation of CD44 with CD3 leads to preferential localization and enhanced phosphorylation of ζ in the insoluble fraction***
IP12-7 cells were stimulated for 10 min at 37 ¡C on plates coated with control IgG (10 g/ml) or anti-CD44 (IM7, 10 g/ml) alone, or anti-CD3 (10 g/ml)plus either control IgG or anti-CD44 (IM7). At the end of the incubation period cells were lysed and ζ was immunopreciptiated from soluble and insoluble fractions as described in materials and methods. Immunoprecipitates were resolved by 12.5% reducing SDS-PAGE and analyzed by anti-phosphotyrosine immunoblotting (upper panel). The lower panel shows the same blot stripped and reblotted with anti-ζ. The positions of nonphosphorylated ζ (p18) and phosphorylated ζ (pp21 and pp23) are indicated. The detection of Ig (light chain), due to binding of the secondary-HRP conjugated antibody is also shown.

Taken together, CD3/CD44 coengagement results in a profound upregulation of early TCR-induced tyrosine phosphorylation events, including phosphorylation of $p95^{vav}$, PLCγ and LAT, and in an increased activation of the TCR proximal protein tyrosine kinase ZAP-70. Moreover, coligation of CD44 with CD3 enhances the level of tyrosine phosphorylation of TCR components and specifically targets them to the cytoskeleton. Thus, these data clearly demonstrate that CD44 functionally cooperates with the TCR during the earliest phases of the signaling cascade and indicate that the costimulatory function of CD44 proceeds by enhancing/facilitating TCR signaling.

3.4 CD44 is associated with src-family protein tyrosine kinases

As efficient ITAM phosphorylation and ZAP-70 activation is often dependent on the recruitment of src family protein tyrosine kinases by coreceptors and/or accessory molecules (Wiest et al., 1996; Alberola-Ila et al., 1997) the potential association of CD44 with protein kinases was investigated. To this end, CD44 was immunoprecipitated from Brij-58 lysates and the immunoprecipitates were subjected to an *in vitro* kinase assay. Phosphorylated proteins were analyzed by SDS-PAGE, followed by Western blotting and autoradiography. Proteins of a molecular weight of about 40, 55-60, 70 and 85-95 kD were found to be highly phosphorylated in CD44 immunoprecipitates of IP12-7 cells (Figure 26A; left panel). A similar pattern of phosphorylated proteins was observed when CD44 was precipitated from detergent lysates of thymocytes (Figure 26A; right panel). Reprecipitation of the *in vitro* phosphorylated proteins of CD44 immunoprecipitates with an anti-phosphotyrosine specific mAb revealed that predominantly protein tyrosine kinases account for the associated kinase activity (Figure 26C). Importantly, the src family protein tyrosine kinases $p59^{fyn}$ and, to a lower extend, $p56^{lck}$ could be specifically detected in the CD44 immunoprecipitates (Figure 26B, C). The 85-95 kD phosphoprotein does not appear to be $p95^{vav}$, as anti-vav did not precipitate it. Furthermore, the phosphorylated protein of about 40 kD did not react with anti-erk (Figure 26C).

IP12-7 cells were also metabolically labeled with [^{35}S]methionine, lysed and CD44 was immunoprecipitated with specific mAbs. The immunoprecipitated proteins were separated by SDS-PAGE, electroblotted and analyzed by autoradiography. In addition to the CD44 band and a band in the range of the src family kinases, a clear band around 32 kD was detected in the CD44 immunoprecipitates (Figure 27). This 32 kD protein seems to be constitutively associated with CD44 in IP12-7 cells, as well as in thymocytes, since the interaction existed in unstimulated cells and could not be significantly influenced by cross-linking of CD44 or stimulation with PMA or pervanadate (data not shown). Until now, the identity of this novel CD44 associated protein of 32 kD is unknown. An approach to identify the protein by specific coimmunoprecipitation with CD44, silverstaining of two-dimensional gels and subsequent nanoelectrospray tandem mass sectrometric sequencing of the corresponding protein spot is in progress.

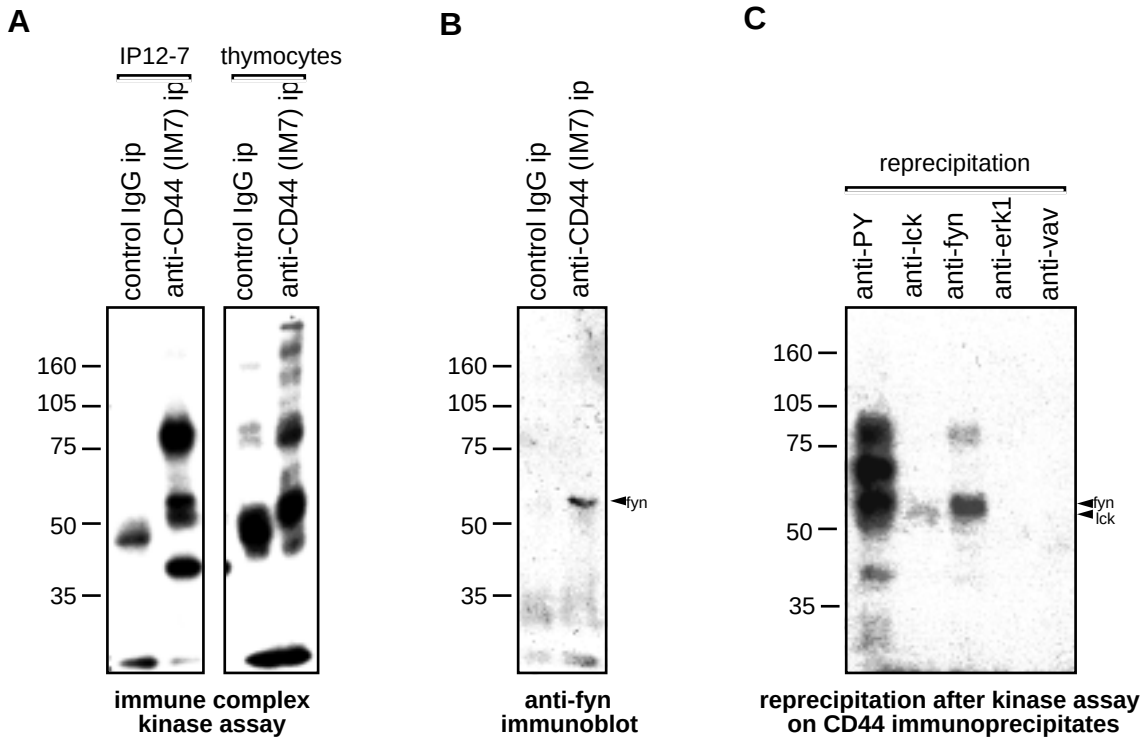

Figure 26: ***CD44 is associated with the src-family protein tyrosine kinases p56^{lck} and p59^{fyn}***
IP12-7 cells (A, left panel; B; C) and thymocytes (A, right panel), respectively, were lysed in IP-buffer containing 1% Brij-58. After preclearing, the lysates were immunoprecipitated with anti-CD44 (IM7) or control IgG. (A) Immunoprecipitates (ip) were analyzed by *in vitro* kinase assay followed by 7.5% reducing SDS-PAGE, electroblotting and autoradiography. (B) Control- and CD44-immunoprecipitates from Brij-58 lysates of IP12-7 cells were resolved by 7.5% reducing SDS-PAGE and analyzed by anti-fyn immunoblotting. (C) After kinase assay on CD44-immunoprecipitates from Brij-58 lysates of IP12-7 cells, the immune complexes were dissociated by SDS, and reimmunoprecipitated using the indicated antibodies. The immunoprecipitated proteins were separated by 7.5% reducing SDS-PAGE, electroblotted and visualized by autoradio-graphy. Positions of molecular weight markers are shown in kD.

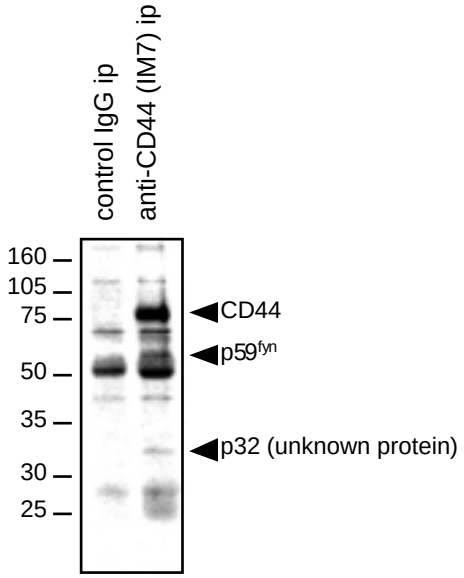

Figure 27

Figure 27 (previous page): ***Coimmunoprecipitation of a 32-kD protein with CD44***
IP12-7 cells were metabolically labeled with [^{35}S]-methionine and [^{35}S]-cysteine and lysed in modified RIPA buffer containing 1% Brij-58. After preclearing, the lysates were immunoprecipitated with control IgG or anti-CD44 mAb. Immunoprecipitates (ip) were resolved by 10% reducing SDS-PAGE, electroblotted and analyzed by autoradiography. The positions of CD44, p59^{fyn} and a unknown 32-kD protein are indicated by arrowheads. Molecular weight markers are shown in kD.

The association of CD44 with src family kinases was analyzed in greater detail by reverse precipitations using an antiserum against p59^{fyn}. As shown in Figure 28, a small amount of CD44 could be specifically detected in anti-fyn immunoprecipitates of Triton X-100 lysates of IP12-7 cells. Fyn and other src related protein tyrosine kinases have been described to be concentrated in detergent-insoluble glycolipid-enriched microdomains (GEMs) (Brown and London, 1997; Simons and Ikonen, 1997). When IP12-7 cells were solubilized by the combination of 0.2% saponin and 1% Triton X-100, which solubilizes GEMs, significantly more p59^{fyn} could be immunoprecipitated (Figure 28; lower panel) and, most importantly, the amount of CD44 present in the anti-fyn immunoprecipitates was found to be dramatically increased, as compared to solubilization in 1% Triton X-100 only (Figure 28; upper panel). Control precipitations with normal rabbit IgG did neither contain p59^{fyn} nor CD44. Saponin is a cholesterol-depleting agent which destabilizes GEM structures rendering them sensitive to detergents such as Triton X-100 (Draberova et al., 1996; Schroeder et al., 1998). Therefore, these data suggest that in T cells a fraction of CD44 constitutively associates with p59^{fyn} in glycolipid-enriched membrane microdomains.

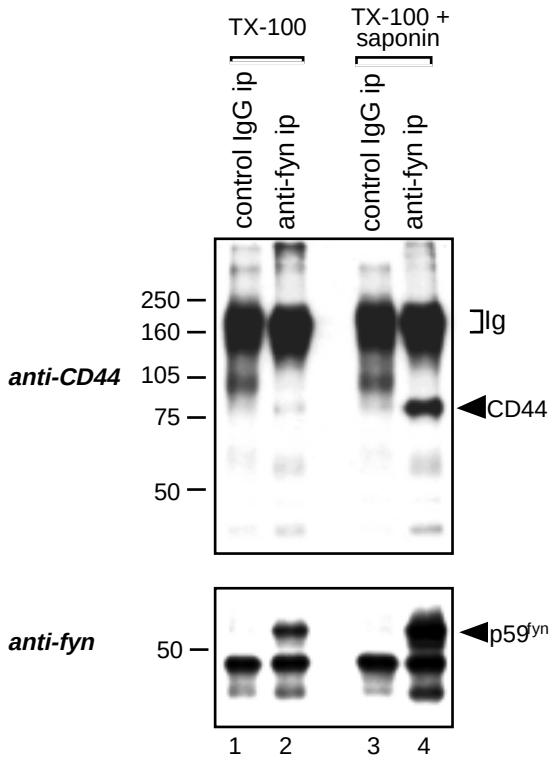

Figure 28: ***Coimmunoprecipitation of CD44 with p59^{fyn}***
IP12-7 cells were detergent solubilized by 1% Triton X-100 (lanes 1-2) or 1% Triton X-100 plus 0.2% saponin (lanes 3-4). The resulting lysates were precleared and afterwards immunoprecipitated with either control IgG or anti-fyn Ab. Immunoprecipitates (ip) were resolved by 7.5% non-reducing SDS-PAGE and immunoblotted with anti-CD44 (IM7) mAb (upper panel). The lower panel shows the same blot stripped and reprobed with anti-fyn Ab. The positions of CD44 and p59^{fyn} are indicated by arrowheads. The detection of Ig, due to binding of the secondary-HRP conjugated antibody is also shown. Molecular weight markers are shown in kD.

3.5 Redistribution of src family kinases into glycolipid-enriched microdomains (GEMs) upon cross-linking of CD44

In T cells a number of important signaling molecules, including src family kinases, have been shown to localize to detergent insoluble glycolipid-enriched microdomains (GEMs), either constitutively or following T cell stimulation. Rearrangement of this so called lipid rafts has recently been identified as a novel component of accessory molecule function (Moran and Miceli, 1998; Viola et al., 1999). As a CD44-dependent translocation of src family protein tyrosine kinases to a Triton X-100 resistant cell fraction has been described in lymphoid cells (Rozsnyay, 1999) and CD44 seems to associate with p59^{fyn} in the detergent insoluble lipid rafts, it was investigated whether cross-linking of CD44 redistributes p59^{fyn} to the GEMs. To address this issue, IP12-7 cells were stimulated on plates coated with either anti-CD44

(IM7) or control IgG. After solubilization in 1% Triton X-100, the lysates were subjected to density sucrose gradient ultracentrifugation to separate the low density GEM fractions from Triton-soluble fractions. 12 gradient fractions were collected from the top to the bottom and each fraction was subsequently analyzed by SDS-PAGE followed by immunoblotting using anti-phosphotyrosine antibody and antibodies against individual proteins. As shown in Figure 29A, in unstimulated cells the major tyrosine phosphorylated proteins in the low density GEM fractions (fractions 2 to 4) had a molecular weight of approximately 60 kD, which is consistent with previous reports (Montixi et al., 1998; Xavier et al., 1998). Interestingly, upon stimulation with anti-CD44 (IM7) the intensity of tyrosine phosphorylation of pp60 in the GEMs significantly increased (Figure 29A). Stripping the same blot and reprobing with anti-fyn revealed that the amount of fyn in the GEM fractions was increased following cross-linkage of CD44 (Figure 29B). Moreover, pp60 and fyn were found to migrate with exactly the same mobility in the polyacrylamide gel, strongly suggesting that fyn is identical to pp60. Anti-fyn immunoprecipitation studies of GEM and Triton-soluble fractions indeed identified fyn as being the tyrosine phosphorylated protein of ~60 kD, which is redistibuted into the GEMs upon engagement of CD44 in IP12-7 cells (Figure 29C). It is worthwhile noting that cross-linking of CD44 specifically targets fyn into the lipid rafts, but apparently doesn't alter the overall phosphorylation state of the enzyme, as the increase in the amount of fyn exactly correlated with the increase in tyrosine phosphorylation. The src like protein kinase $p56^{lck}$ was also found to be translocated to the low density lipid rafts upon engagement of CD44 (data not shown). In unstimulated IP12-7 cells a small proportion of CD44 was associated with the buoyant lipid microdomains, as evidenced by immunoblotting with anti-CD44 (Figure 30A). Importantly, the CD44-mediated increase of fyn and lck in the GEM fractions was accompanied by a similar increase of CD44 in these fractions. GEM purification was confirmed by dot blot immunostainings of the gradient fractions with cholera toxin B, which binds to the GM1 glycosphingolipid. GM1 was specifically detected in the low density fractions (Figure 30B).

Taken together, the data indicate, that in T cells engagement of CD44 triggers its redistribution into glycolipid-enriched membrane microdomains. CD44 recruitment is accompanied by the accumulation of src family tyrosine kinases in GEMs. As the formation of GEM-dependent signaling complexes plays a central role in T cell activation, the CD44-mediated redistribution of signaling molecules into lipid rafts might represent a mechanism by which CD44 can increase TCR signaling processes.

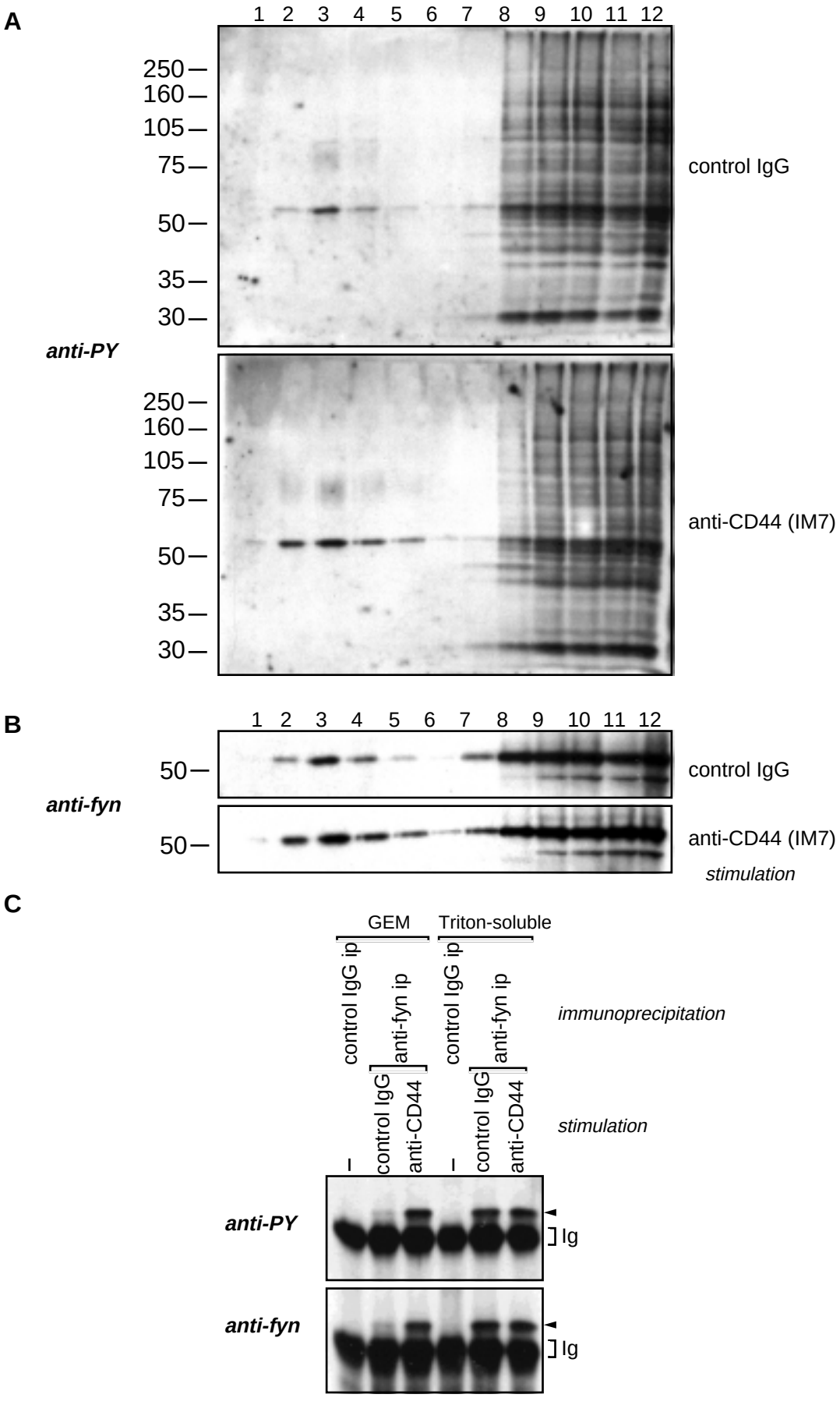
A
1 2 3 4 5 6 7 8 9 10 11 12
250
160
105
75
50
35
30
anti-PY
control IgG
anti-CD44 (IM7)
B
anti-fyn
control IgG
anti-CD44 (IM7)
stimulation
C
GEM
Triton-soluble
control IgG ip
anti-fyn ip
immunoprecipitation
–
control IgG
anti-CD44
stimulation
anti-PY
anti-fyn
Ig

Figure 29 (previous page)
Cross-linking of CD44 induces the redistribution of p59^{fyn} into glycolipid-enriched microdomains
IP12-7 cells were stimulated for 15 min at 37 ¡C on plates coated with either anti-CD44 (IM7, 10 g/ml) or control IgG (10 g/ml). Cells were extracted in TNE buffer containing 0.5% Triton X-100, and the lysates were subjected to sucrose gradient ultracentrifugation. Twelve fractions were collected from the top. (A) Fractions were resolved by 7.5% reducing SDS-PAGE and immuno-blotted with anti-phosphotyrosine mAb. The same blot was stripped and reprobed with anti-fyn (B). Fyn was immunoprecipitated from GEM-fractions (pooled fractions 2-4) and Triton X-100 soluble fractions (pooled fractions 10-12) from detergent lysates of IP12-7 cells stimulated for 15 min with immobilized anti-CD44 (IM7, 10 g/ml) or control IgG (10 g/ml). Immunopreciptitates were resolved by 7.5% reducing SDS-PAGE and analyzed by anti-phosphotyrosine immuno-blotting (C, upper panel). The same blot was stripped and reprobed with anti-fyn (C, lower panel). The position of fyn is indicated on the right. The detection of Ig, due to binding of the secondary-HRP conjugated antibody is also shown. Molecular weight markers are shown in kD.

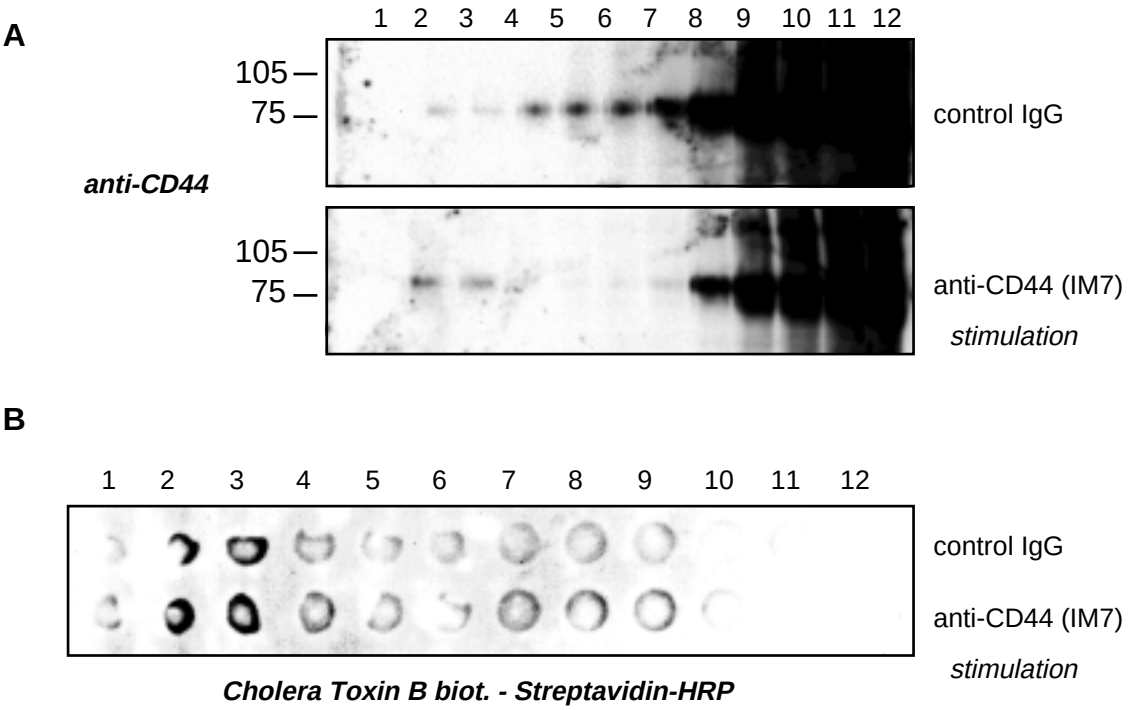

Figure 30: ***Distribution of CD44 in glycolipid-enriched microdomains of IP12-7 cells***
IP12-7 cells were stimulated for 15 min at 37 ¡C on plates coated with either anti-CD44 (IM7, 10 g/ml) or control IgG (10 g/ml). Cells were extracted in TNE buffer containing 0.5% Triton X-100, and the lysates were subjected to sucrose gradient ultracentrifugation. Twelve fractions were collected from the top. (A) Fractions were resolved by 7.5% non-reducing SDS-PAGE and immunoblotted with anti-CD44 mAb (IM7). Molecular weight markers are shown in kD. (B) Sucrose gradient fractions were dot-blotted and GM1 was detected by reaction with cholera toxin B.

3.6 CD44 engagement induces cytoskeletal rearrangements in T cells

A functional actin cytoskeleton is an essential prerequisite for a variety of different T cell activities, such as migration, homing and interaction with APCs. The accumulation of F-actin at the interface of the T cell and the APC has been suggested to stabilize and favour continuous TCR-antigen interactions (Valetutti et al., 1995). Furthermore the actin cytoskeleton may provide a scaffold for the spatial distribution of mechanistic and signaling components required for physiologic T cell function. Since CD44 has been reported to be associated with cytoskeletal complexes (Geppert and Lipsky, 1991; Bourguignon et al., 1992; Tsukita et al., 1994) it was investigated whether engagement of CD44 could induce actin cytoskeletal rearrangements in T cells.

T cell activation is accompanied by the polarized reorganization of the cytoskeleton and the asymmetric clustering of receptors and signaling molecules, referred to as caps. To study a possible role of CD44 in the polarization/organization of the actin cytoskeleton in T cells, CD44 receptor caps were induced on IP12-7 cells. To this end, cells were incubated with anti-CD44 mAb (IM7) followed by cross-linking of the primary antibody using FITC-labeled anti-rat IgG. After fixation, F-actin was visualized by phalloidin-TRITC staining. As demonstrated by the formation of strong F-actin accumulations at the site of the CD44 receptor caps (Figure 31), clustering of CD44 on IP12-7 cells sufficed to induce the polarization of cortical actin cytoskeletal elements.
As members of the rho family of small GTPases (e.g. rho, rac1, and cdc42) play a crucial role in the regulation of actin cytoskeletal structures (Hall, 1998), they were considered as potentially involved candidates in the CD44-mediated changes of the actin cytoskeleton. Immunofluorescence stainings revealed that rac1 was clearly colocalized with CD44 receptor caps (Figure 32). In contrast, neither rho nor cdc42 were found to be significantly accumulated at the site of CD44 caps.

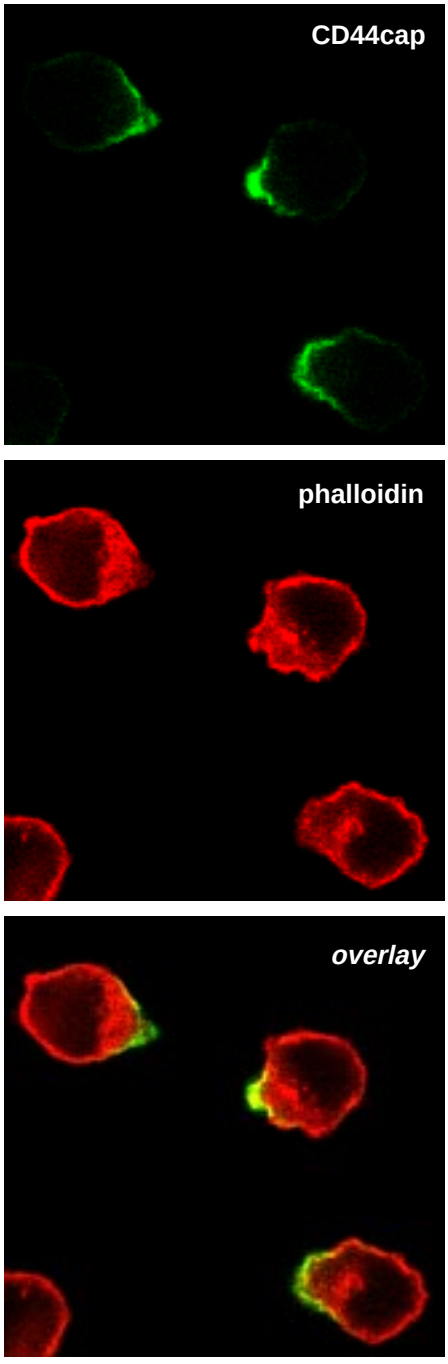

Figure 31: ***Accumulation of F-Actin at the site of CD44 receptor caps***
CD44 receptor caps were induced by incubating IP12-7 cells for 15 min with soluble anti-CD44 (IM7, 10 g/ml). Primary antibodies were cross-linked for 30 min at 37 ¡C using FITC-conjugated secondary antibodies. After fixation, cells were permeabilized and F-actin was visualized by staining with phalloidin-TRITC. Samples were analyzed with a confocal laser scanning microscope. CD44 caps are shown in green. Red fluorescence indicates F-actin. A digital overlay of red and green fluorescence is shown in the lower panel.

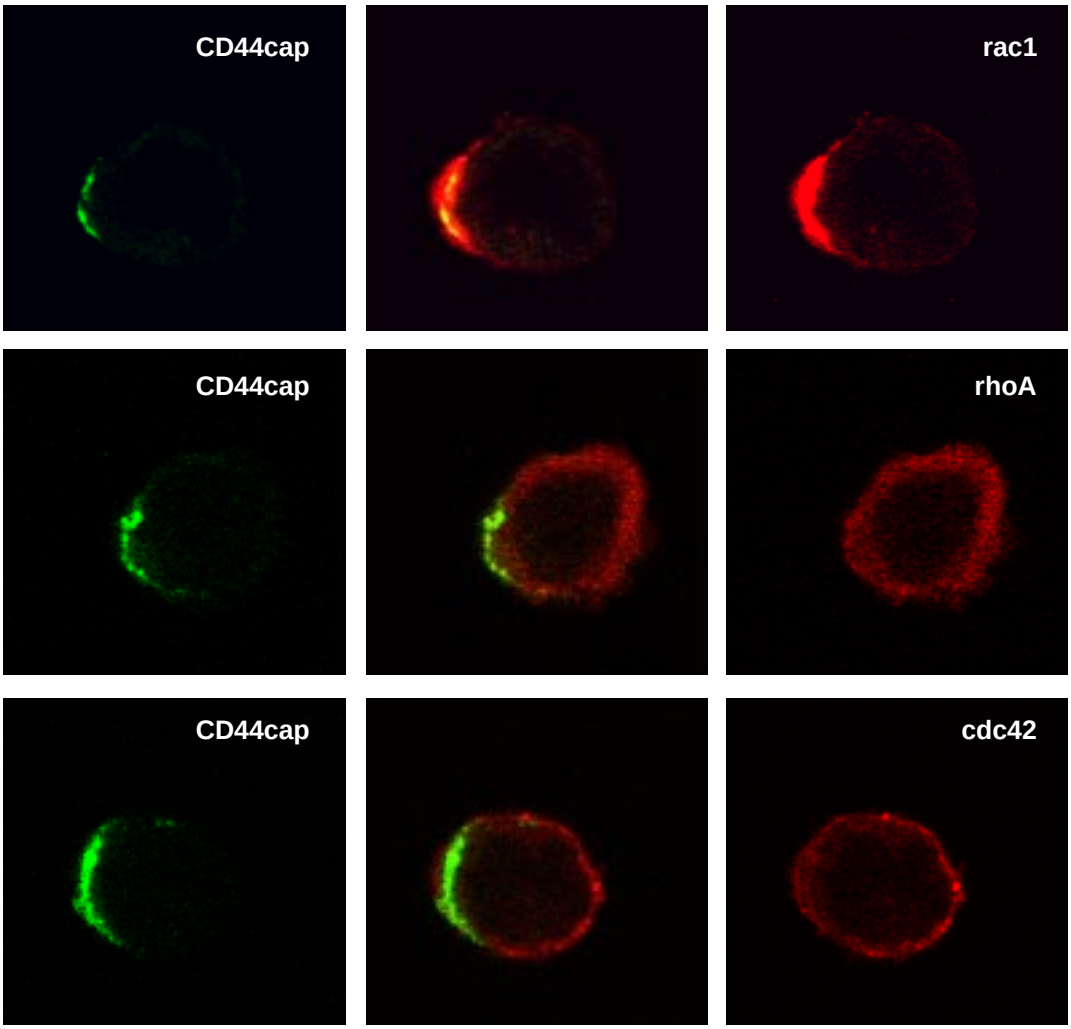

Figure 32: ***Rac1 colocalizes with CD44 receptor caps***
CD44 receptor caps were induced by incubating IP12-7 cells for 15 min with soluble anti-CD44 (IM7, 10 g/ml). Primary antibodies were cross-linked for 30 min at 37 ¡C using FITC-conjugated secondary antibodies. Cells were fixed and permeabilized as described in materials and methods. The subcellular localization of rac1, rhoA, and cdc42 was revealed by indirect immuno-fluorescence staining employing specific primary antibodies and Texas-red-conjugated secondary antibodies. CD44 caps (green, left panels) and rac1, rhoA, and cdc42 (red, right panels) were analyzed with a confocal laser scanning microscope. Digital overlays of red and green fluorescence are shown in the middle panels to show colocalization.

In a next set of experiments it was elaborated whether triggering via CD44 could also induce cell adhesion and spreading, which are highly important processes for T cells and involve dynamic rearrangements of the actin cytoskeleton. In the absence of stimulation IP12-7 cells do not adhere to culture plates and exhibit spherical morphology. However, when plated onto anti-CD44 (IM7) coated dishes, IP12-7 cells displayed a dramatic change in morphology characterized by strong adhesion, flattening and cell spreading. Notably, the induction of a spread phenotype was dependent on the epitope recognized by the CD44-specific antibody, i.e. was not observed with KM81 (Figure 33). To further analyze the phenomenon of CD44-mediated cell spreading and to investigate whether actin polymerization is involved, IP12-7 cells were cultured for various periods of times on IM7-coated plates. Thereafter, the cells were fixed and subsequently stained with phalloidin-TRITC, which specifically binds to F-actin. As revealed by immunofluorescence microscopy, within minutes the cells adhered to IM7-coated surfaces and then spread over a period of ~1 hour (Figure 34). During this period, cells flattened and developed various surface protrusions. This process which was accompanied by a complex reorganization of the actin cytoskeleton, as characterized by the formation of F-actin bundles. Pretreatment of the cells with cytochalasin B, an agent which disrupts the actin cytoskeleton, completely inhibited cell spreading (Figure 33). These data demonstrate that CD44-mediated cell spreading is dependent on a functional actin cytoskeleton. Interestingly, IP12-7 cells pretreated with nocodazole, an microtubule depolymerizing factor, did not spread on coated IM7, indicating also the involvement of the microtubular system in CD44-induced cell flattening and spreading. The morphological changes induced by CD44 were energy dependent, since they were neither observed by incubating the cells at 4¡ C, nor after treating the cells with 2-deoxyglucose-azide, an energy depleting system (Figure 33).

Since src-family kinases, as well as PI3-kinase, have been implicated in adhesive processes and cell spreading (Meng et al., 1998), the role of these kinases in CD44-induced morphological changes was investigated. The involvement of src-kinases could be demonstrated by the finding that pretreatment of IP12-7 cells with different concentrations of the src-kinase inhibitor pp2 (Hanke et al., 1996) reduced CD44-mediated cell spreading in a dose dependent manner (Figure 33 and 35). In contrast, the pharmacological inhibitors of PI3-kinase LY294002 (25 M) and wortmannin (100 nM) did not inhibit the ability of IP12-7 cells to spread on coated IM7 (Figure 33). Also, pretreatment of the cells with ocadaic acid, an inhibitor of type 1 and 2 serine phosphatases, had no effect on CD44-mediated cell spreading. These data indicate that src-kinase activity is functionally involved in the signaling pathway that regulates CD44-mediated cytoskeletal rearrangements and subsequent morphological changes, whereas neither PI3-kinase nor serine phosphatases of type 1 and 2 seem to be required for these processes.

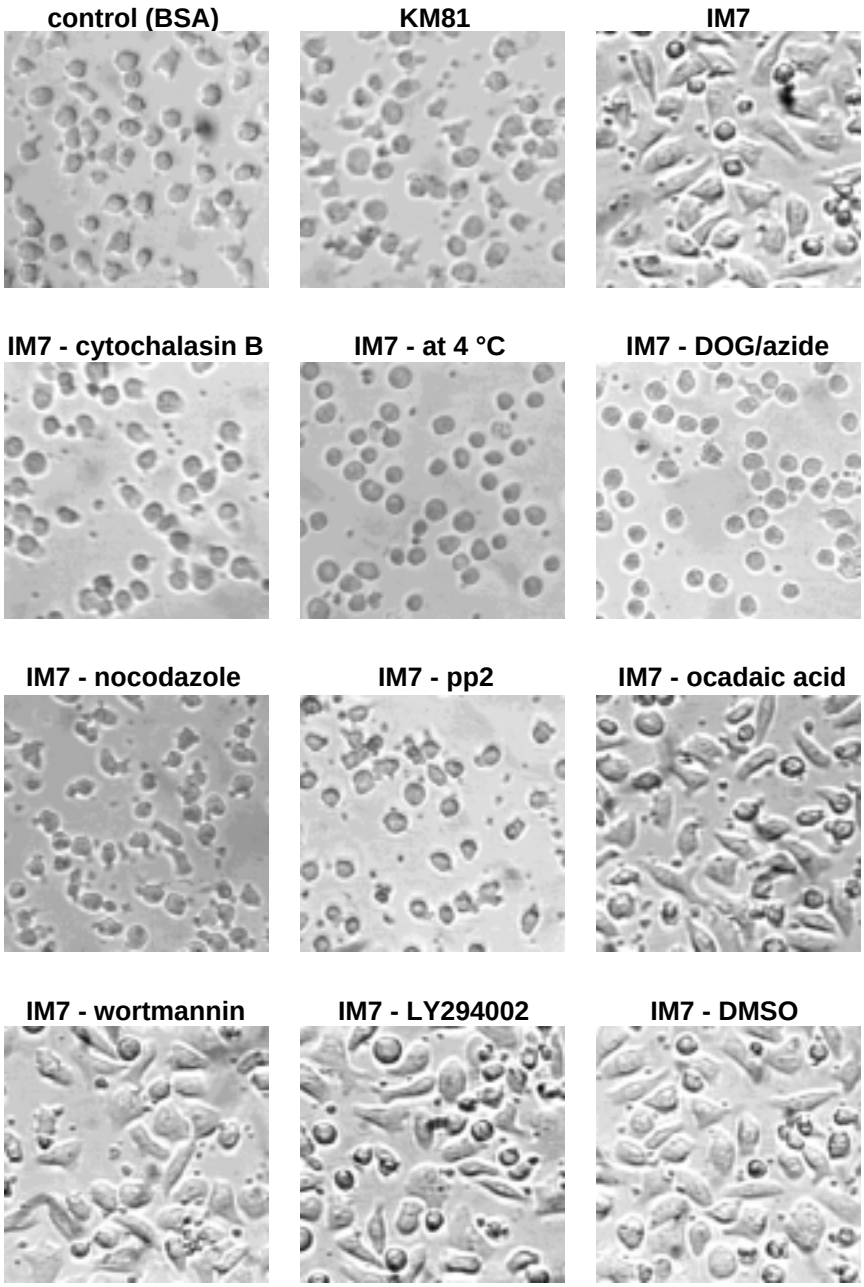

Figure 33: ***Effects of pharmacological inhibitors on CD44-mediated cell spreading***
IP12-7 cells were pretreated for 20 min at 37 ¡C with 50 mM 2-deoxyglucose-0.04% sodium azide (DOG/azide), cytochalasin B (1 g/ml), nocodazole (1 M), pp2 (80 M), wortmannin (100 nM), LY294002 (50 M), ocadaic acid (0.5 M) and carrier DMSO and seeded on plates coated with anti-CD44 (IM7). As controls, cells were added to plates coated with anti-CD44 (KM81) or BSA. After incubation for 1 hour at 37 ¡C or 4 ¡C, respectively, cells were visualized with a light microscope and photographed.

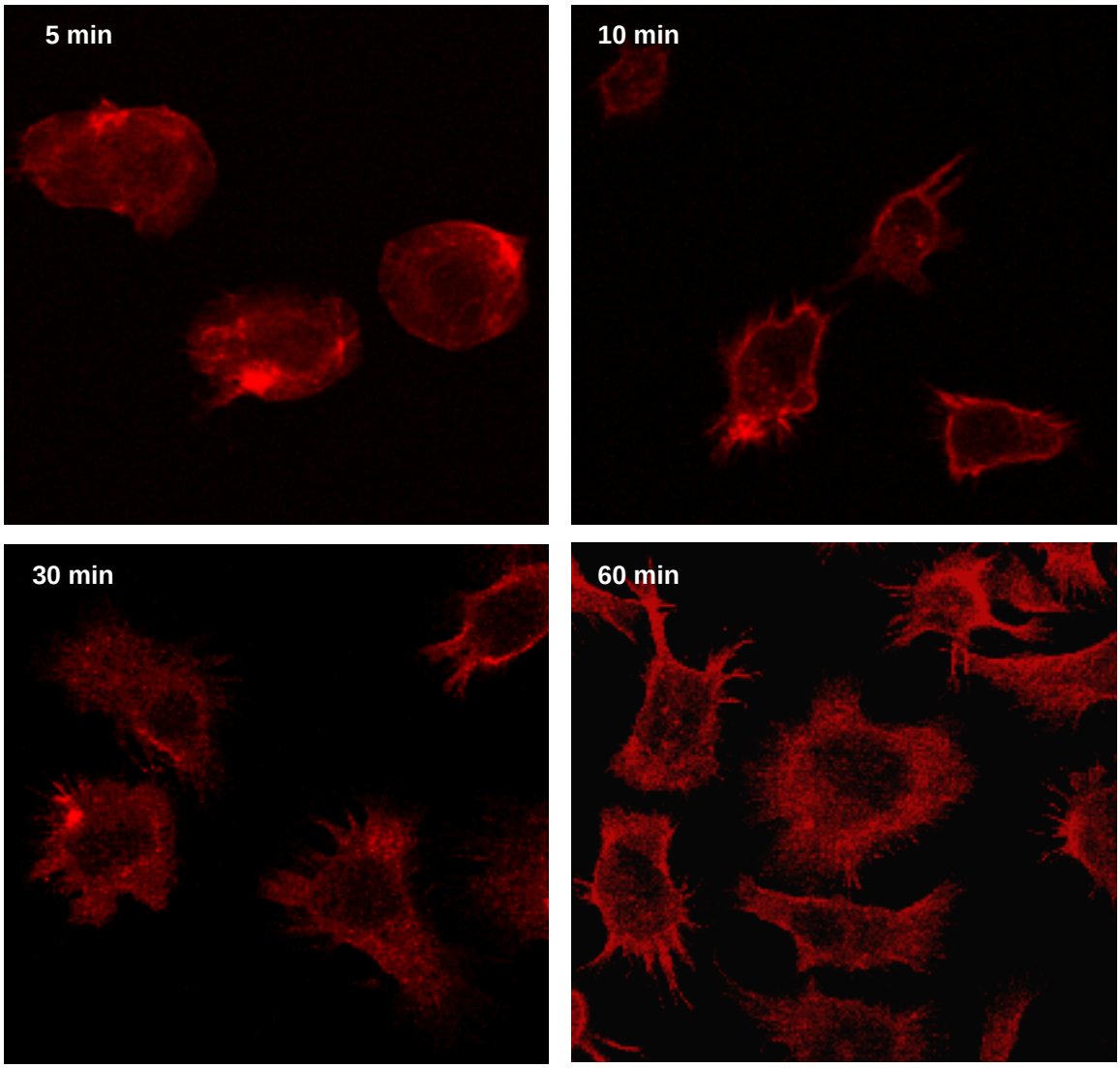

Figure 34: ***CD44-mediated cell spreading and cytoskeletal rearrangements***
IP12-7 cells were seeded on plates precoated with 10 g/ml anti-CD44 (IM7). Cells were incubated at 37 ¡C for the indicated period of time. After fixation, cells were permeabilized and F-actin was stained with phalloidin-TRITC (shown in red) as described in materials and methods. Cells did not spread on dishes coated with poly-L-lysine (data not shown). Digitized images were generated using a confocal laser scanning microscope.

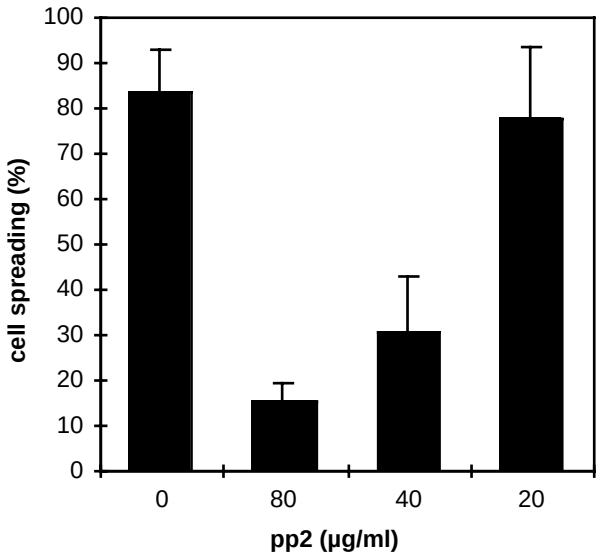

Figure 35: ***The src-kinase inhibitor pp2 reduces CD44-mediated cell spreading in a dose dependent mannner***
IP12-7 cells were pretreated for 20 min at 37 ¡C with various concentrations of pp2 and seeded on plates coated with anti-CD44. After incubation for 1 hour at 37 ¡C, the cells were visualized by phase contrast microscopy and scored for the percentage of spread cells.

To gain additional insight in the signaling elements involved in CD44-induced cytoskeletal changes, IP12-7 cells were incubated on IM7-coated dishes to induce cell spreading. Cells were fixed after 1 hour and the distribution of small GTPases of the rho subfamily was studied by immunofluorescence staining using specific antibodies. As shown in Figure 36, CD44 induced cell spreading was accompanied by the formation of punctate spots of rac1 around the cell margin. In contrast, rho and cdc42 were not specifically located to the cell periphery but were rather equally distributed throughout the cytoplasm.
In view of the observation that triggering of CD44 induced cell spreading and specifically targeted rac1 to the leading edge of the cell, the potential role of rac1 in CD44-induced cytoskeletal rearrangements was further explored. To this end, IP12-7 cells were transiently transfected with expression plasmids encoding myc-tagged dominat negative mutant forms of rac1 and rho kindly provided by Mark Simons (ONYX), i.e., myc-racN17 and myc-rhoN19, respectively, and their ability to influence CD44-mediated morphological changes was accessed. Expression of these mutant proteins was confirmed by anti-myc epitope immunoblotting (Figure 38). Cells were cultured for 1 hour on dishes coated with anti-CD44 mAbs (IM7). After fixation, transfected cells expressing the mutants were detected with anti-

myc mAb 9E10 and costained with phalloidin-TRITC, to visualize F-actin (Figure 37). Control cells and untransfected cells exhibited the characteristic spread phenotype with numerous surface extensions and the formation of actin bundles. Overexpression of myc-rhoN19 did not significantly interfere with CD44-induced cell spreading, although the formation of actin bundles was sometimes less clear as compared to control cells. Cells expressing dominant negative rac1 (myc-racN17) displayed a round phenotype and failed to spread on IM7-coated culture plates. Expression of myc-racN17 also blocked the formation of F-actin fibres in transfected IP12-7 cells, indicating that rac1 is required for CD44-mediated cytoskeletal rearrangements leading to cell spreading.

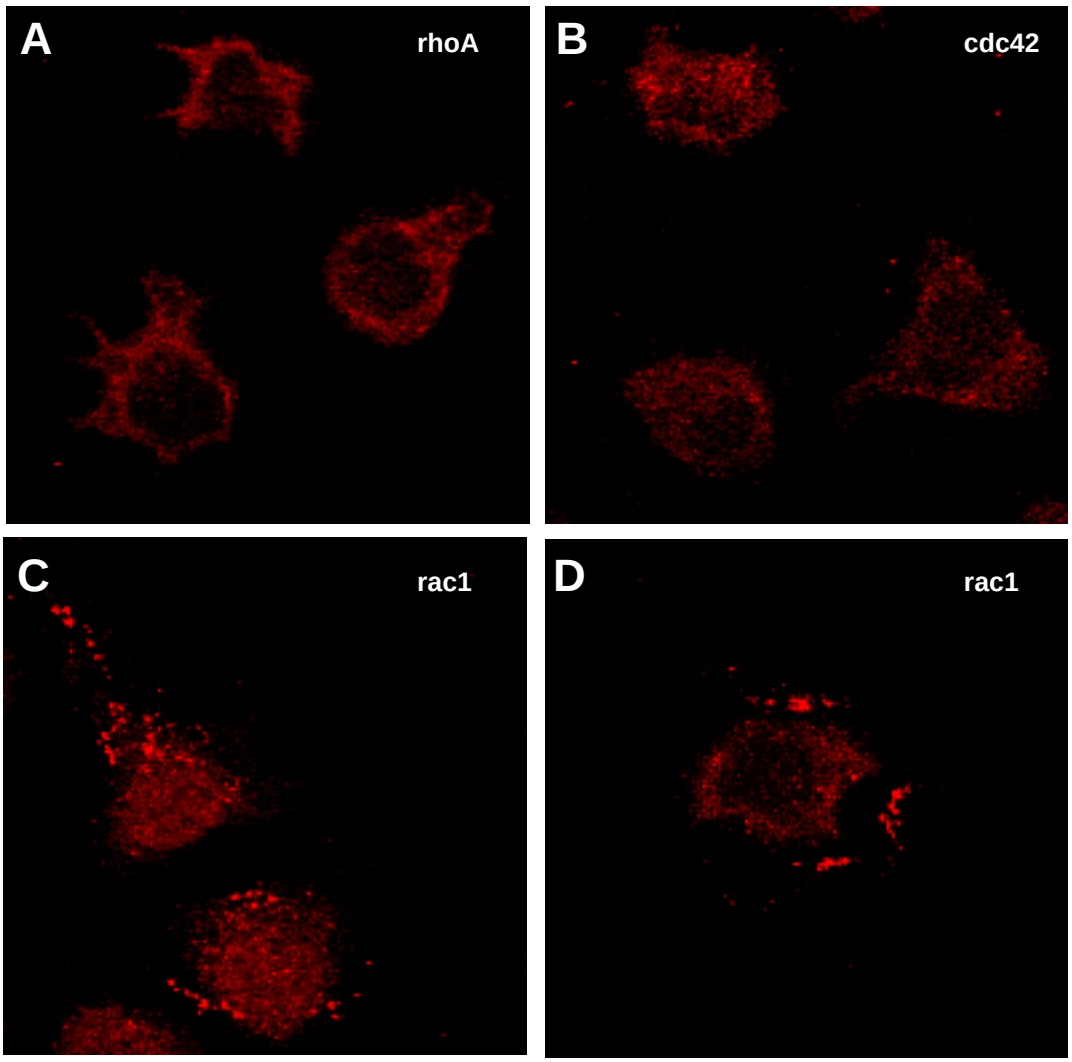

Figure 36: ***Distribution of small rho-family GTPases in IP12-7 cells cultured on anti-CD44-coated plates***
IP12-7 cells were cultured for 60 min on plates coated with 10 g/ml anti-CD44 (IM7). Cells were fixed, permeabilized and subsequently the subcellular localization of rhoA (A), cdc42 (B), and rac1 (C, D) was revealed by indirect immunofluorescence staining using specific primary antibodies and Texas-red-conjugated secondary antibodies. Digitized images were generated using a confocal laser scanning microscope.

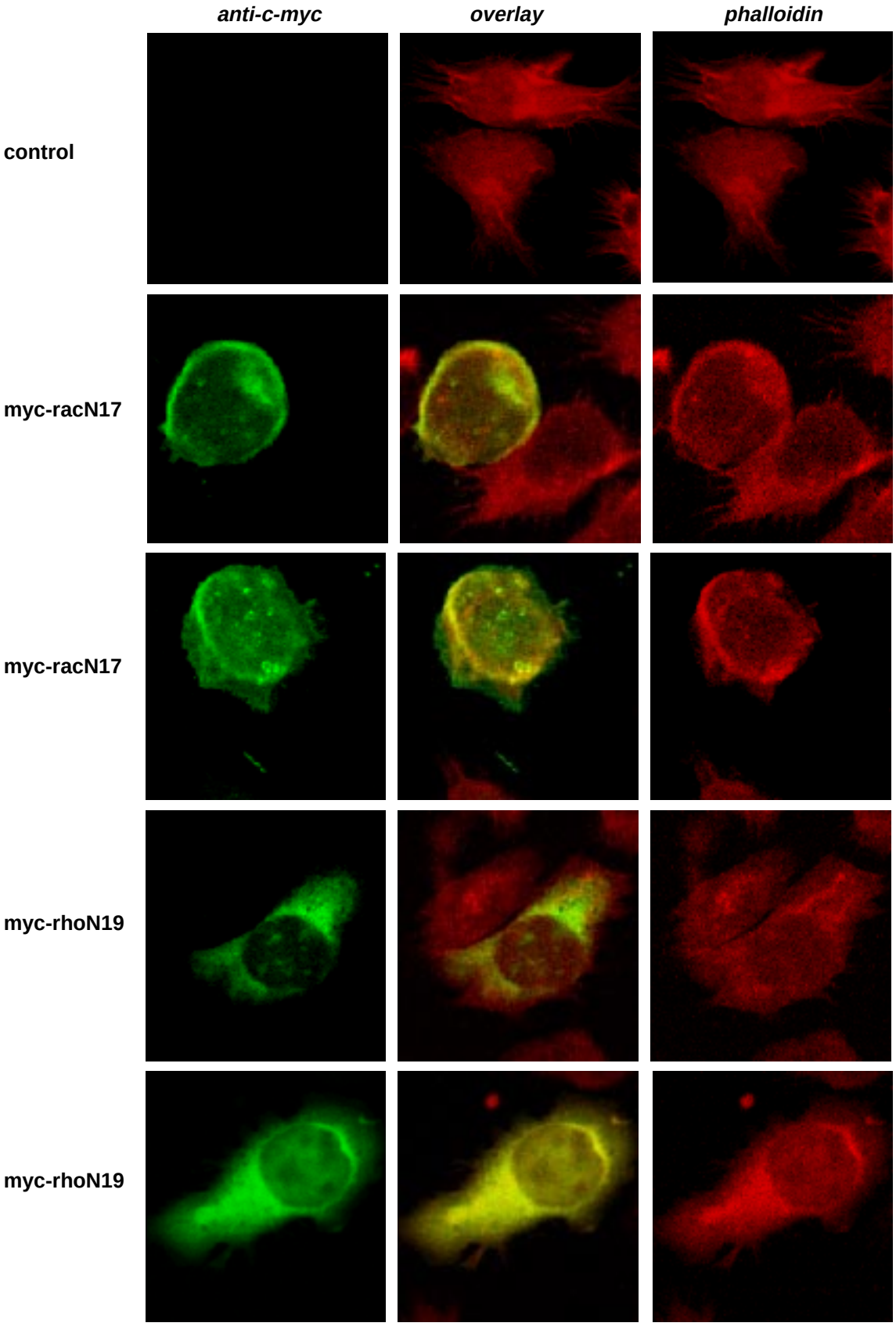
anti-c-myc
overlay
phalloidin
control
myc-racN17
myc-racN17
myc-rhoN19
myc-rhoN19

Figure 37

Figure 37 (previous page): ***Effect of racN17 and rhoN19 on CD44-mediated cell spreading***
IP12-7 cells were transiently transfected with expression plasmids encoding myc epitope-tagged dominant negative mutant forms of rac1 (myc-racN17) and rhoA (myc-rhoN19), respectively. 16 h after transfection, the cells were seeded on plates coated with 10 g/ml anti-CD44 (IM7) and incubated for 60 min at 37 ¡C. Cells were fixed and permeabilized as described in materials and methods. Transfected cells were detected by immunofluorescence staining using anti-c-myc mAb 9E10 and Cy2-conjugated secondary Ab (shown in green, left panels). F-actin was visualized by staining with phalloidin-TRITC (shown in red, right panels). The digital overlays of red and green fluorescence are shown in the middle panels.

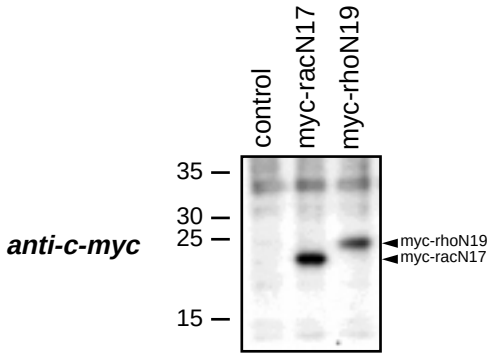

Figure 38: ***Expression of myc-racN17 and myc-rhoN19 in transiently transfected IP12-7 cells***
IP12-7 cells were transiently transfected with myc-racN17 and myc-rhoN19, respectively. 16h after transfection, dead cells were removed by Ficoll density centrifugation and the living cells were lysed in RIPA buffer containing 1% Triton X-100. Lysates were resolved by 10% reducing SDS-PAGE and immunoblotted with anti-c-myc mAb (9E10). Positions of myc-racN17 and myc-rhoN19 are indicated by arrowheads. Molecular weight markers are shown in kD.

Taken together, these data demonstrate that independently of other stimuli triggring via CD44 can induce morphological changes associated with strong adhesion, cell flattening and cell spreading. The spread phenotype is dependent on an intact actin cytoskeleton and also involves the microtubular system. The CD44 signaling pathway leading to cytoskeletal rearrangements requires src-family kinase activity, but seems to be independent of PI3-kinase. Moreover, rac1, a small GTPase of the rho family, is functionally involved in the transduction of extracellular signals to the cytoskeleton leading to CD44-induced cell spreading. It is worthwhile noting that, similarly to the results on the co-induction of lymphocyte activation, the CD44-induced morphological changes were only observed with the CD44 specific antibody IM7. As the cytoskeleton is more and more emerging as an integral component of lymphocyte activation, the CD44-induced cytoskeletal rearrangements in T cells might not only have implications for migration and homing processes, but also might play an important role for the costimulatory function of CD44.